Index

Brochures:

Published Papers:

Fuel Cells R&D: Enhancing Performance through Pore Structure

Pore Structure Characteristics Governing Performance of Fuel Cells

One of the critical factors which determine the performance of fuel cells is the pore structure characteristic of many of the fuel cell components such as membranes, GDLs, separators, and electrodes. Pore structure governs the flow and the kinetics of the physio-chemical processes which occur in the fuel cell. The pore structure characteristics, important and relevant for fuel cell components are pore diameter, pore throat diameter, pore volume, pore distribution, graded pore structure, surface area, external surface area, total porosity, hydrophobic and hydrophilic nature of pores in a mixture, liquid and gas permeability, and diffusional flow. In a working fuel cell, the chemical environment, the operating temperature, the humidity, and the stresses generated during the operation can considerably alter the pore structure. Therefore, not only the determination of pore structure characteristics is important, evaluation of the influence of stress, temperature, and chemical environments on structural characteristics is also relevant.

Techniques for Measurement of Pore Structure Characteristics

Following techniques can be used for evaluation of pore structure characteristics of fuel cell components.

Capillary Flow Porometry

Measures a wide range of through pore diameters, pore distribution, and gas permeability over a range of temperatures, stresses, and chemical environments including variable humid atmospheres.

Liquid Extrusion Porosimetry

Measures through pore volumes, diameters and distribution over a range of temperatures, stresses, and chemical environments including variable humid atmospheres. Can measure hydrophobic through pores as well as hydrophilic through pores. In a mixture, the characteristics of hydrophobic and hydrophilic through pores can also be determined.

Capillary Condensation Flow Porometry

Measures through nanopore diameter, distribution, and flow rate without any structural distortion due to pressure or temperature.

Permeametry

Measures gas, vapor, and liquid transmission rates of many chemical species over a wide range of temperatures, pressures, and concentrations.

Vacuapore

It is a water intrusion porosimeter and it measures through and blind pore hydrophobic pore volume, diameter and distribution. Characteristics of hydrophobic and hydrophilic pores in a mixture can be determined in combination with mercury intrusion porosimetry.

Mercury Intrusion Porosimetry

Measures through and blind pore volume, diameter and distribution.

BET Sorptometry

Measures surface area, very small through and blind pore volume, distribution, chemisorptions of many chemicals over a wide range of temperatures and pressures.

Pycnometry

Measures true and bulk density of materials.

How Can PMI Help?

Porous Materials, Inc. is a company that designs, manufactures, and sells instruments for pore structure characterization. The company has vast experience in patenting of novel technology for pore structure characterization and developing custom instruments for a wide variety of applications. We have published many papers and presented many oral and poster papers in conferences on pore structure characterization of fuel cell and battery components. Some of these papers may be found in our website. We have supplied instruments to many fuel cell and battery related industries and research laboratories.

All the instruments needed for pore structure characterization of fuel cell components are manufactured by us. Our **Fuel Cell Porometer** is specially designed for fuel cell components. In all our instruments, test execution, data acquisition, data storage, and data reduction are fully automated. Windows-based menu driven operation of the instrument is very simple to use. The results are objective, accurate, and reproducible.

We also have our in-house contract testing laboratory. We have tested fuel cell components of many customers from a wide variety of organizations including fuel cell companies, universities, and research organizations.

.

Example of Application of PMI Instruments:
Pore Structure Characterization of Toray Paper

The Toray paper, a carbon coated material, is extensively used in fuel cell industry. The PMI pore structure characterization instruments measured the very interesting pore structure characteristics of the Toray paper.

Volume of Different Kinds of Pores

Different functions of fuel cell components are governed by different kinds of pores. Volume of three different kinds of pores in Toray paper was measured by PMI instruments and is illustrated in Figure 1. The instruments used for these measurements are summarized below.

(i) Volume of the through pores: Measured by PMI Liquid Extrusion Porosimeter

(ii) Volume of through and blind pores: Measured by PMI Mercury Intrusion Porosimeter

(iii) Volume of through and blind hydrophobic pores: Measured by PMI Non-Mercury Water Intrusion Porosimeter

Through pores constitute about 75 % of the pore volume. About 25 % of the pore volume is due to blind pores. Hydrophobic pore constitute 29 % of pore volume and 71 % of the pore volume is due to hydrophilic pores.

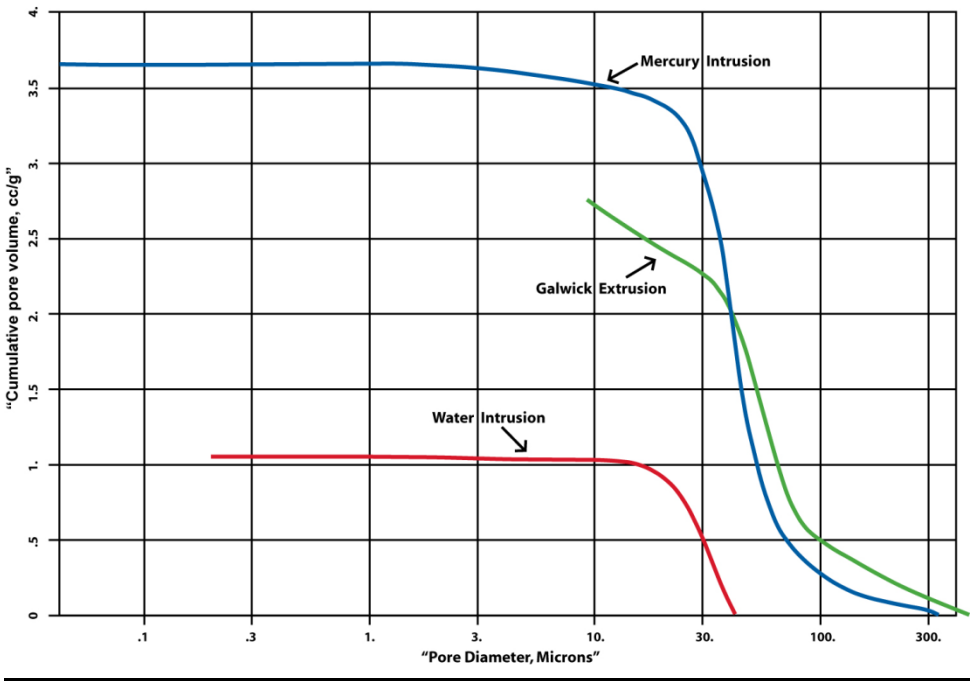

Figure 1. Pore volume of different kinds of pores

Pore Volume Distribution of Different Kinds of Pores

The measured pore volume distribution (Figure 2) shows how the three different types of pores (through and blind pores, through pores, and hydrophobic pores) are distributed. The differences between the peaks can be used to estimate the distribution of blind pores and hydrophilic pores. The median pore diameters of various kinds of pores are shown in Table I. It is apparent that the through pores are primarily hydrophilic while the blind pores are primarily hydrophobic. The hydrophilic through pores can also be measured by *PMI* Water Extrusion Porosimeter.

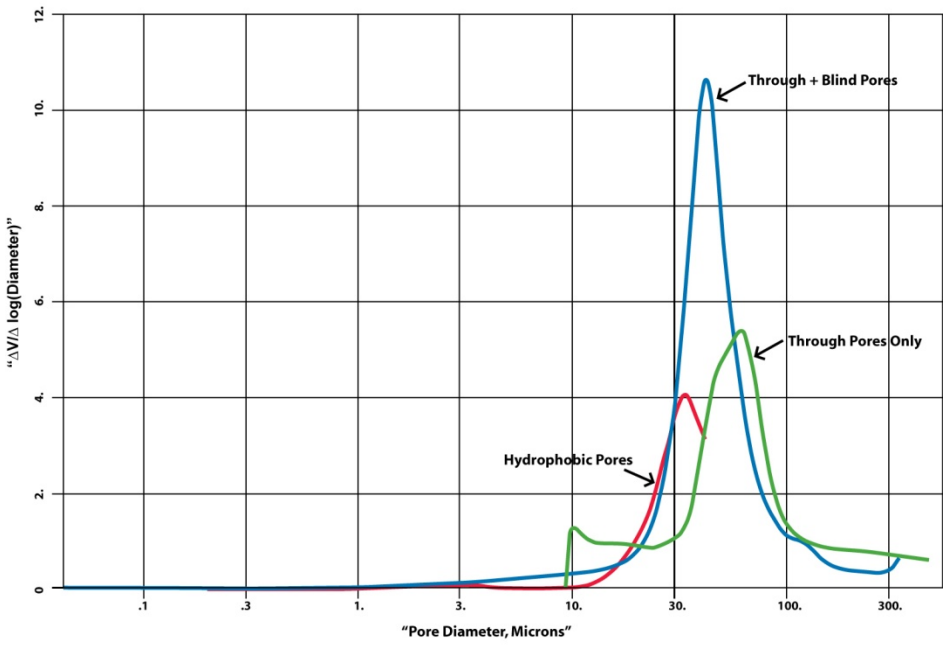

Figure 2. Distribution of different types of pores

Table I Pore Structure Characteristics

Characteristics	Through Pores	Blind Pores	Hydrophobic Pores	Hydrophilic Pores
% Pore Volume	75 %	25 %	29 %	71 %
Median Pore Diameter	60 μm	40 μm	35 μm	50 μm
Kind of Pore	Hydrophilic	Hydrophobic	Blind Pores	Through Pores

Characteristics of Through Pores Responsible for Fluid Flow

Pore throat diameters determine the flow rate of fluid through the through pores and the restrictions for passage of large particles through the through pores. Characteristics of pore throat diameters of through pores can be determined by PMI Capillary Flow Porometer.

This technique measures the largest pore throat diameter, the mean flow pore throat diameter, and the pore distribution. The pore distribution is in Figure 3. The pore throat characteristics of through pores are listed Table 2.

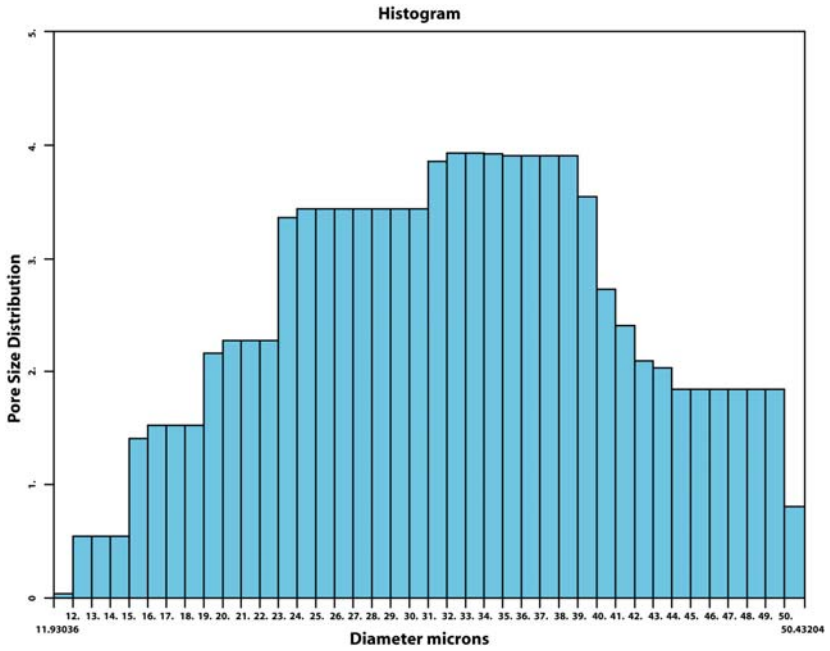

Figure 3. Distribution of through pore throat diameters

Table 2. Characteristics of Through Pores

Characteristics	Values
The Largest Throat Diameter	50.43 μm
Mean Flow Throat Diameter	32.48 μm
Range of Throat Diameters	20 - 45 μm
Change of Pore Diameter Along Pore Length	Small
Median Pore Diameter based on Volume	60 μm
Volume of Pores	75 %
Nature of pores	Hydrophilic

The distribution plot shows that most of the through pore throat diameters are in the range of 20 to 45 μm. Comparison of these value with the diameters of through pores based on volume

measurements (Figure 3 and 4) shows that the shapes of through pores are not like hour glasses. The through pore diameters do not change appreciably along the pore length and are similar in magnitude.

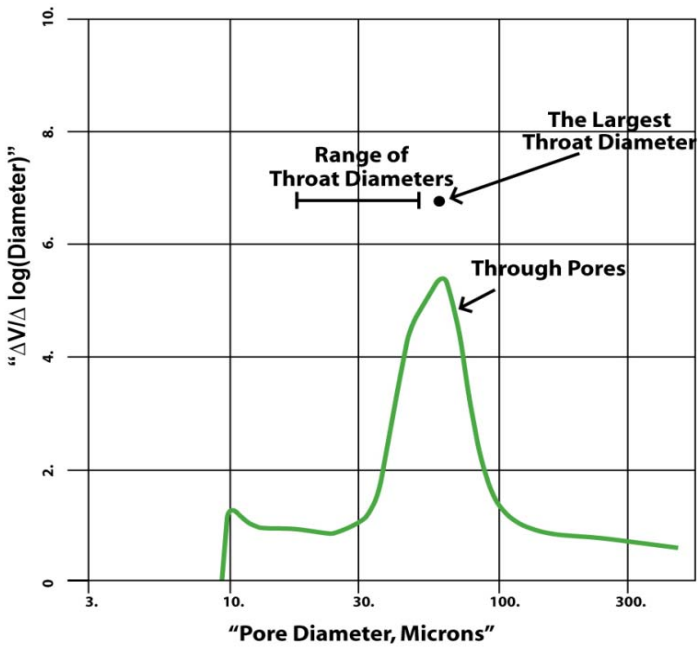

Figure 4. Pore throat diameters and volume based pore diameters of through pores

Special Needs

You can visit our website to see the wide spectrum of pore structure capability that our instruments offer. If you have a special need that is not part of PMI's standard test list, the engineers at PMI will be happy to talk to you about your testing requirements and come up with a suitable solution. Please free to contact us:

Porous Materials, Inc.
20 Dutch Mill Rd
Ithaca, NY 14850

Ph: 607-257-5544
Toll Free (US & Canada): 1-800-825-5764
Fax: 607-257-5639

Online: www.pmiapp.com
Email: info@pmiapp.com

Fuel Cell Porometer

Description

The PMI Fuel Cell Porometer provides fully automated through-pore analysis including pore-throat diameter, pore size distribution, mean flow pore diameter, and liquid & gas permeability. The porometer's versatility allows the user to simulate operating conditions. The instrument has special features to measure the effects of compressive stress on a sample, test temperature, sample orientation, and layered structure on pore structure characteristics. The fully automated, user-friendly Fuel Cell Porometer is an asset in quality control and R&D environments.

Principle

The flow rate of an inert gas through the dry sample is measured with increasing pressure. The sample is brought in contact with a wetting liquid, the liquid spontaneously fills the pores in the sample, and the flow through the wet sample is measured with increasing differential pressure.

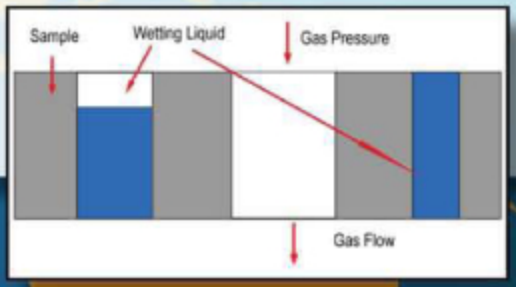

Features

Measured flow rates through dry and wet samples with increasing differential pressure are used to compute many characteristics.

- Pore throat diameters
- The largest pore throat diameter
- Mean flow pore diameter
- Pore distribution
- Gas permeability
- Through pore surface area (Envelope Surface Area)

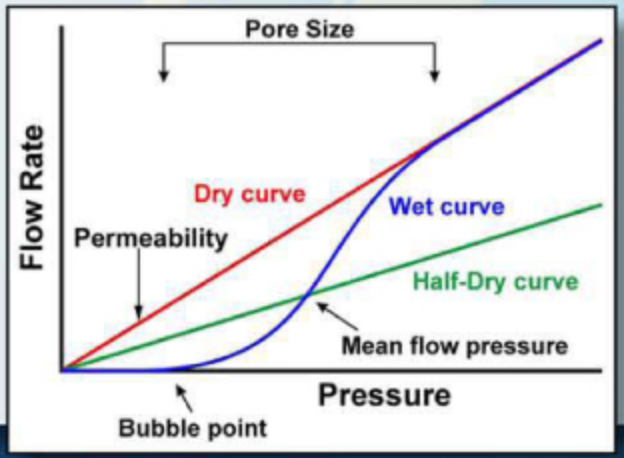

Unique Features

- Characteristics measureable using gas with 0 to 100 % humidity
- Test temperatures can be 200°C and in special situations 800°C
- Pore size measured in samples under compressive stress of up to 1000 psi
- Pore structure of each layer of a multilayer composite
- Pore diameters down to about 0.013 µm

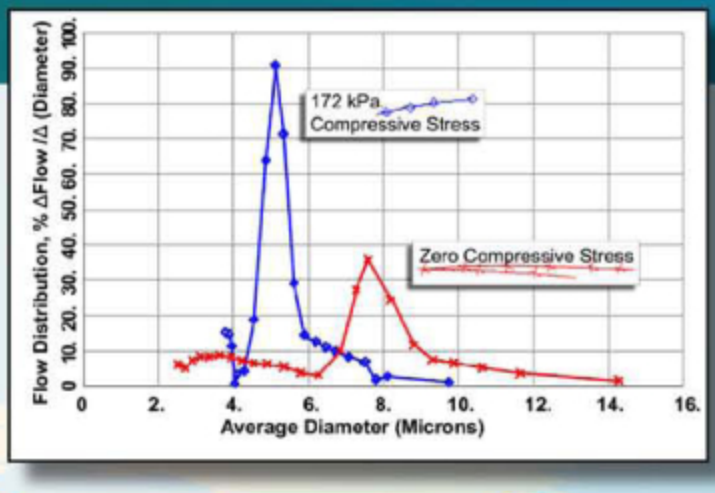

Applications

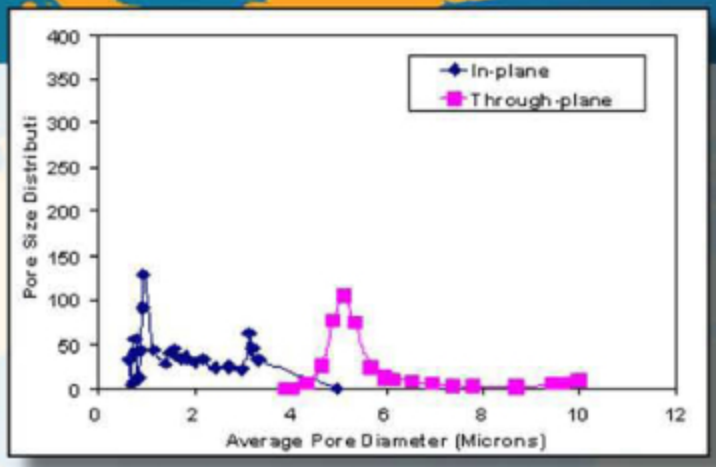

The performance of many fuel cell components is determined primarily by the characteristics of the pore structure. Flow of reactants and products is determined by the pore size and pore distribution of electrodes, wide range of gas humidity found in many applications can change the pore structure, components subjected to compressive stress during operation can considerably modify the pore size, pore structure of each layer of multilayer composites often used as fuel cell components can determine the performance of the fuel cell, and reaction rate of reactants is governed by the surface area of through pores. The Fuel Cell Porometer is designed to measure all the relevant pore structure characteristics of fuel cell components.

Other Products

Bubble Point Tester
Capillary Flow Porometer
Capillary Condensation Flow Porometer
Clamp-On Porometer
Complete Filter Cartridge Analyzer
Compression Porometer
Custom Porometer
Cyclic Compression Porometer
Envelope Surface Area Analyzer
Filtration Media Analyzer
High Flow Porometer
Integrity Analyzer
In-Plane Porometer
Microflow Porometer
Nanopore Flow Porometer
QC Porometer
Average Fiber Diameter Analyzer
Diffusion Permeameter
Gas Permeameter
Liquid Permeameter
Vapor Permeameter
Water Vapor Transmission Analyzer
Liquid Extrusion Porosimeter
Mercury/Nonmercury Intrusion Porosimeter
Vacuapore
Water Intrusion Porosimeter (Aquapore)
BET Liquisorb
BET Sorptometer
Gas Pycnometer
Mercury Pycnometer

Also Available:
Testing Services
Consulting Services
Short Courses

Buy Rent Lease

Porous Materials, Inc.
20 Dutch Mill Rd, Ithaca, NY 14850 USA
Tel: (607)-257-5544 Toll Free in USA & Canada: 1-800-TALK-PMI
Fax: (607) 257-5639 Email: info@pmiapp.com WWW.PMIAPP.COM

PMI

Capillary Flow Porometer

Applications

The PMI Capillary Flow Porometer is used for R&D and quality control in industries worldwide such as filtration, nonwovens, pharmaceutical, biotechnology, healthcare, household, food, hygienic products, fuel cells, water purification, and battery. Samples often tested include: filter media, membranes, paper, powders, ceramics, battery separators, and health care products.

Principle

A wetting liquid is allowed to spontaneously fill the pores in the sample and a nonreacting gas is allowed to displace liquid from the pores. The gas pressure and flow rates through wet and dry samples are accurately measured.

The gas pressure required to remove liquid from the pores and cause gas to flow is given by:

$$D = 4 \gamma \cos \theta / p$$

where D is the pore diameter, γ is the surface tension of liquid, θ is the contact angle of liquid, and p is the differential gas pressure. From measured gas pressure and flow rates, the pore throat diameters, pore size distribution, and gas permeability are calculated.

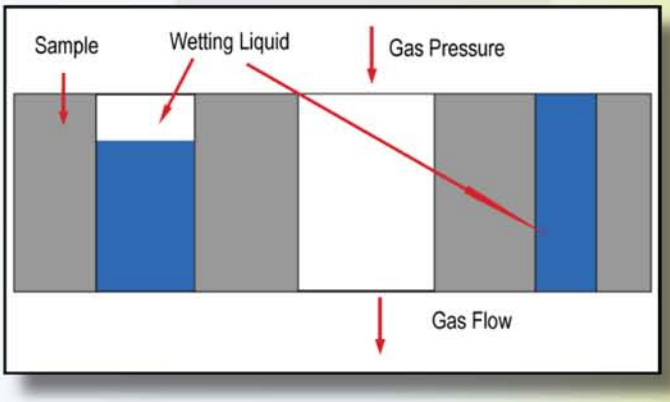

Features

- Testing of small samples as well as complete parts
- Any sample geometry (Example: sheets, rods, tubes, hollow fibers, cartridges, and powders)
- Any nonwetting liquid
- Tests in QC, research, or any number of user defined modes
- See-through sample chamber for visual observation of test available
- Real time graphic display
- Window based software for all control, measurement, data collection,data reduction, and report preparation

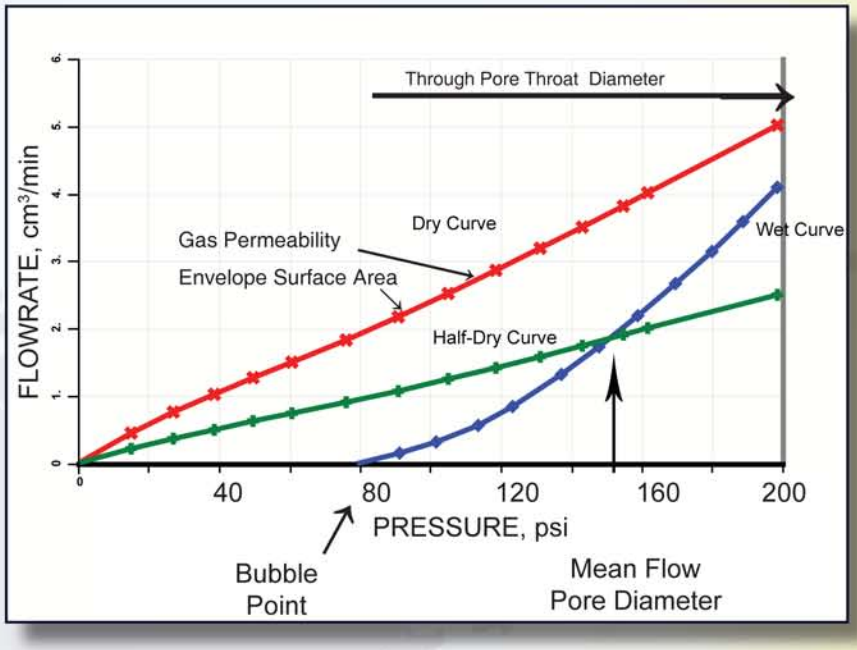

Special Features

- Adjustable pressure on o-rings through pneumatically controlled piston-cylinder device
- Measurement of pressure close to the sample to minimize pressure drop correction
- Straight flow path avoiding turbulence
- Versatile sample chamber for a variety of samples and test modes

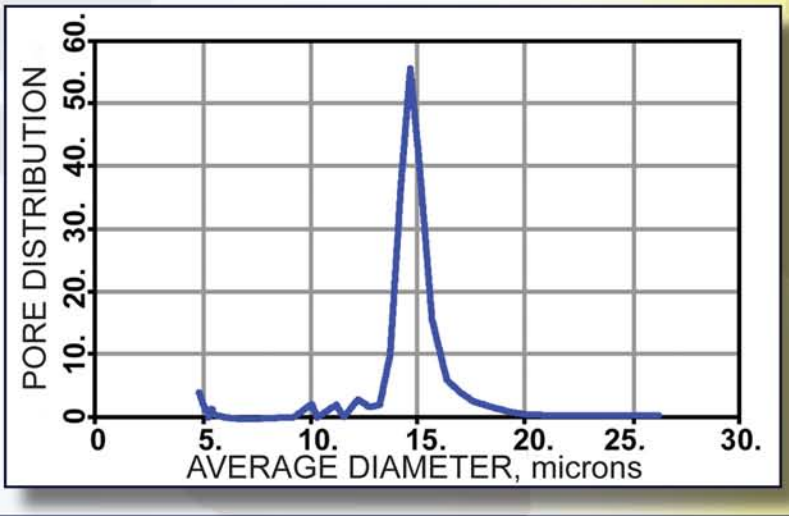

Capabilities

- Diameter of the most constricted part of a through pore (pore throat)
- Bubble point (the largest through pore throat diameter)
- Mean flow pore diameter (50% of flow is through pores smaller than the mean flow pore)
- Pore diameter range
- Pore distribution

  Distribution function f:

  f = -d[(fw/fd) x 100] / dD

  fw = flow rate through wet sample

  fd = flow rate through dry sample
- Gas permeability in many desired units including Frazier, Gurley, Rayle, and Darcy

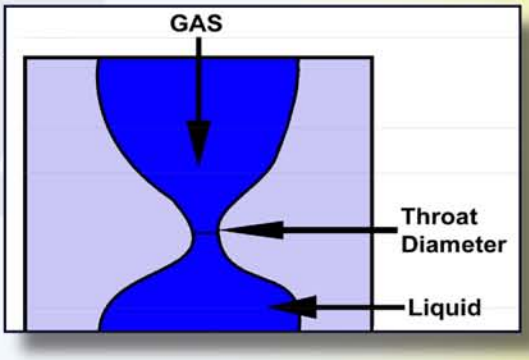

Optional Capabilites

- Liquid permeability: Measuring liquid flow rate through the sample when pressure is applied on excess liquid on the sample. Volume of liquid measured using a penetrometer.
- Pressure Hold Test
- Hydro-head (break through pressure) test
- Integrity test
- Envelope Surface Area, average particle size and average fiber diameter obtained from gas flow rate through dry sample
- Multiple sample chamber
- Multiple test mode
- Shuffled smoothness test
- Burst pressure test
- Use of desired fluid including strong chemicals
- Elevated temperature test

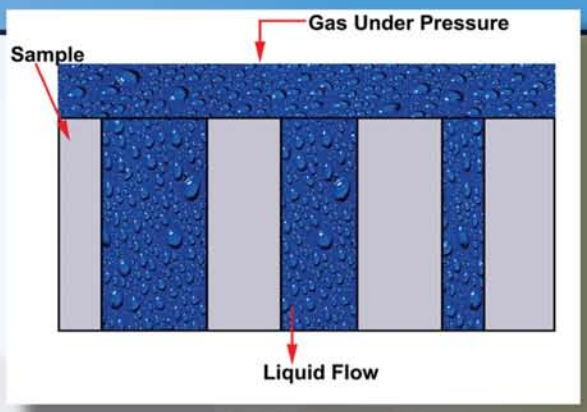

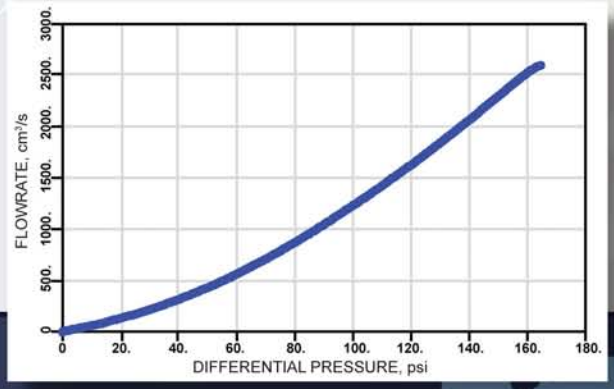

Multi-Mode Instruments

- Q.C., Clamp-On, In-Plane, and Compression modes may be combined
- In-Plane test permits measurement of pore in the x-y plane
- In-plane test permits insitu determination of pore diameter and structure of each layer of the multi-layer media

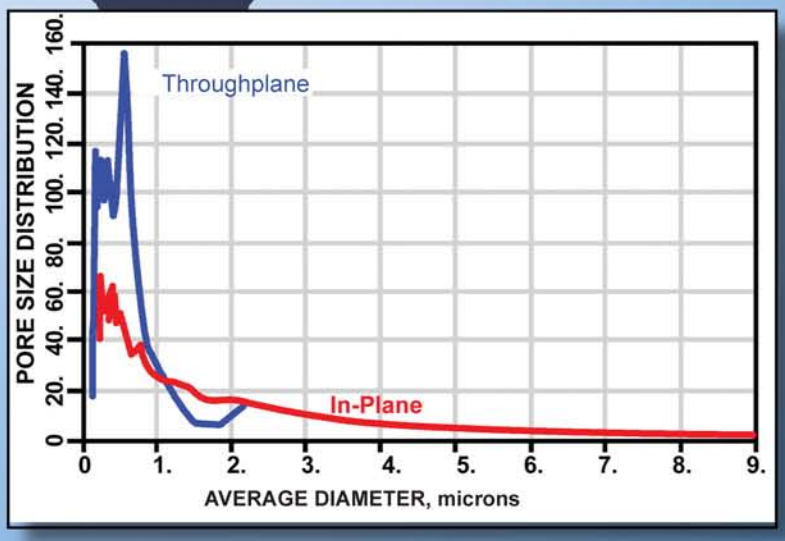

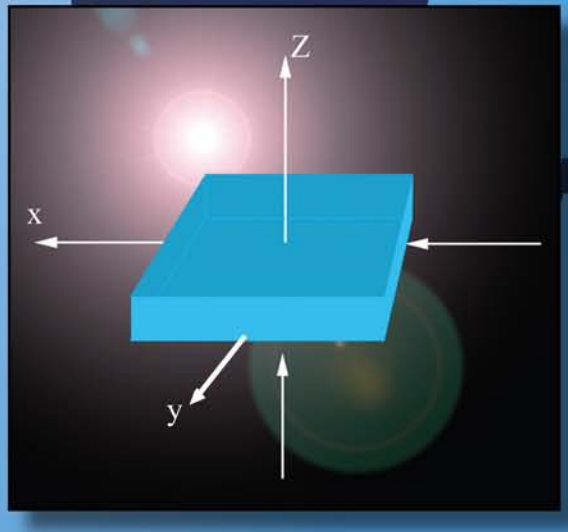

Specifications

Pressure Accuracy: 0.15% of reading

Test Pressure: 100, 200 and 500 psi instrument versions (700, 1400, 3500 kPa instrument versions)

Pressure and Flow Resolution:
1/60,00 of full scale (1 part in 60,000)

Maximum Pore Size Detectable: 500 μm

Minimum Pore Sizes Detectable:

Flow Rates: Up to 200 SLPM (standard liters per minute)

Sample Size:
Standard: 0.25" - 2.5" diameter (up to 1.5 " thick).
Standard: 5 mm - 60 mm diameter (up to 40 mm thick).
Others available

Sample Geometry: Sheets, Rods, Tubes, Hollow Fibers, Cartridges, Powders, etc.

Fluid	Surface Tension, dynes / cm	Diameter μm, (100 psi Porometer)	Diameter, μm, (200 psi Porometer)	Diameter, μm (500 psi Porometer)
Water	72	0.30	0.15	0.06
Mineral Oil	34.7	0.14	0.07	0.03
Petroleum Distillate	30	0.12	0.06	0.03
Denatured Alcohol	22.3	0.09	0.05	0.02
Silwick	20.1	0.08	0.04	0.02
Porewick	16	0.07	0.03	0.014
Galwick	15.9	0.07	0.03	0.014

Other Products

Average Fiber Diameter Analyzer
Bubble Point Tester
Capillary Flow Porometer
Capillary Condensation Flow Porometer
Complete Filter Cartridge Analyzer
Clamp-On Porometer
Compression Porometer
Custom Porometer
Cyclic Compression Porometer
Envelope Surface Area Analyzer
Filtration Media Analyzer
High Flow Porometer
Integrity Analyzer
In-Plane Porometer
Microflow Porometer
Nanopore Flow Porometer
QC Porometer
Diffusion Permeameter
Gas Permeameter
Liquid Permeameter
Vapor Permeameter
Water Vapor Transmission Analyzer
Liquid Extrusion Porosimeter
Mercury/Nonmercury Intrusion Porosimeter
Vacuapore
Water Intrusion Porosimeter (Aquapore)
BET Liquisorb
BET Sorptometer
Gas Pycnometer
Mercury Pycnometer

Also Available:
Testing Services
Consulting Services
Short Courses

Buy Rent Lease

Porous Materials, Inc.
20 Dutch Mill Rd, Ithaca, NY 14850 USA
Tel: (607)-257-5544 Toll Free in USA & Canada: 1-800-TALK-PMI
Fax: (607) 257-5639 Email: info@pmiapp.com WWW.PMIAPP.COM

Liquid Extrusion Porosimeter

Description

The PMI Liquid Extrusion Porosimeter is a unique instrument with the ability to measure through–pore volume, volume distribution and liquid permeability without using mercury. The instrument is employed for characterization of porous materials used in many industries such as biotech, pharmaceutical, filtration, food, and environment. It produces no harmful effects on personnel or environment.

Principle

The sample is placed on a membrane in the sample chamber. The membrane is such that its largest pore is smaller than the smallest pore to be tested. The pores of the sample and the membrane are filled with a weting liquid. The pressure of a nonreacting gas is increased on the sample to extrude the liquid from the pores. The differential pressure, p, required to displace liquid from a pore is related to its diameter, D, surface tension of the liquid, γ, and contact angle of the liquid, θ.

$$p = 4 \gamma \cos \theta / D$$

The displaced liquid passes through the liquid–filled pores of the membrane and its volume is measured, while the liquid-filled pores of the membrane prevent the gas from passing through because of insufficient pressure. The gas pressure gives the pore diameter. The volume of displaced liquid gives the pore volume. Measurement of liquid flow rate without the membrane under the sample yields liquid permeability of the sample.

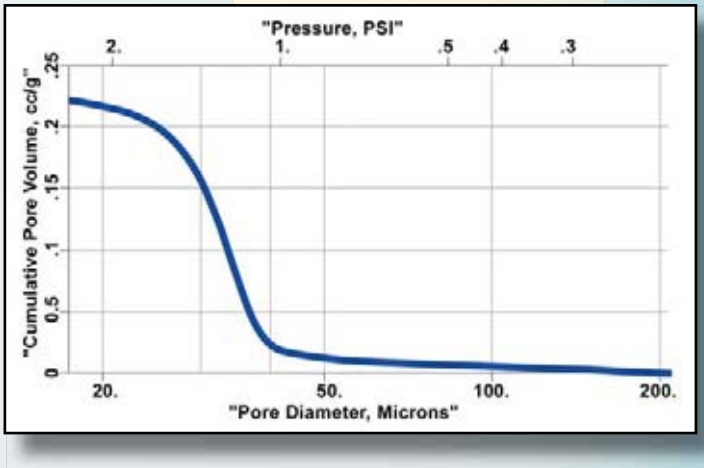

Features

- One Instrument performs like two. Measures liquid permeability like a permeameter and pore volume like a Mercury Intrusion Porosimeter.
- No toxic material like mercury is used.
  No health hazard.
  No disposal-related cost.
- Fully automated. Simple to use.
  Very little operator involvement.
- Highly reproducible & accurate.
- A wide variety of samples can be investigated.
- Pressure required almost an order of magnitude less than that required for mercury intrusion.
- Can be used for pressure sensitive materials.
- Only instrument capable of measuring through-pore volume.
- Effects of application environment measurable. (stress, temperature, chemical environment).
- Capable of measuring very large pores (up to 1000 microns).

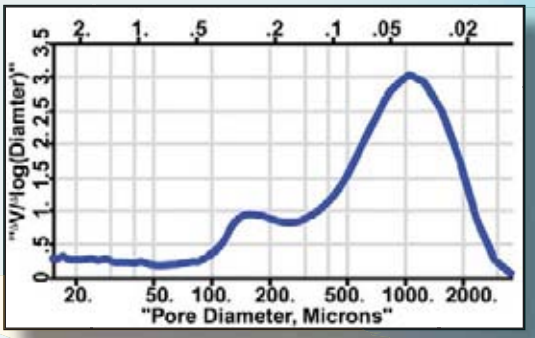

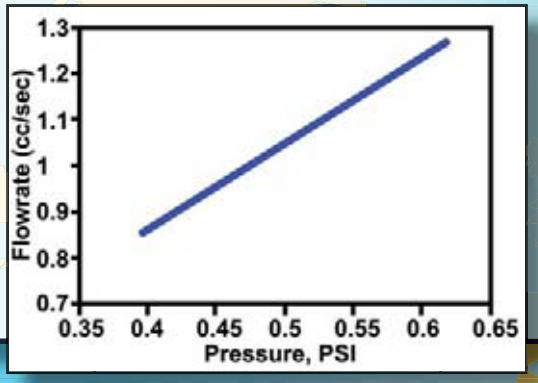

Specifications

Pressure Range
0 - 100 psi (Others Available)

Pore Size Range
1000 μm - 0.05 μm

Resolution
1 in 20,000

Intrusion Volume Range
0.01 cc

Sample Size
1.5” Diameter, 1” Thick
(Others Available)

Other Products

Average Fiber Diameter Analyzer
Bubble Point Tester
Capillary Flow Porometer
Capillary Condensation Flow Porometer
Complete Filter Cartridge Analyzer
Clamp-On Porometer
Compression Porometer
Custom Porometer
Cyclic Compression Porometer
Envelope Surface Area Analyzer
Filtration Media Analyzer
High Flow Porometer
Integrity Analyzer
In-Plane Porometer
Microflow Porometer
Nanopore Flow Porometer
QC Porometer
Diffusion Permeameter
Gas Permeameter
Liquid Permeameter
Vapor Permeameter
Water Vapor Transmission Analyzer
Liquid Extrusion Porosimeter
Mercury/Nonmercury Intrusion Porosimeter
Vacuapore
Water Intrusion Porosimeter (Aquapore)
BET Liquisorb
BET Sorptometer
Gas Pycnometer
Mercury Pycnometer

Also Available:
Testing Services
Consulting Services
Short Courses

Buy Rent Lease

Porous Materials, Inc.
20 Dutch Mill Rd, Ithaca, NY 14850 USA
Tel: (607)-257-5544 Toll Free in USA & Canada: 1-800-TALK-PMI
Fax: (607) 257-5639 Email: info@pmiapp.com WWW.PMIAPP.COM

07/08

Capillary Condensation Flow Porometer

Applications

The PMI Capillary Condensation Flow Porometer has the unique ability to measure gas permeability and flow rate distribution in addition to measuring pore diameter of nanopore samples without using any toxic materials or extreme pressures and temperatures. No other instrument has such capabilities. It is utilized for characterization of porous membranes used in many industries such as biotech, pharmaceutical, filtration, food and environmental without any fear of harmful effects of high pressures and extreme temperatures on samples. Fragile samples with small pores can be easily evaluated by this technique.

Principle

At a given temperature, a vapor at a pressure less than the pressure, Po, of vapor in equilibrium with its liquid can condense in pores of a material. Kelvin equation gives the diameter of the pore in which condensation can occur at the relative vapor pressure, (P/ Po).

$$\ln (P/ Po) = - [(4 g V \cos Q) / (D R T)]$$

where g is the surface tension of condensed liquid, V is the molar volume of condensed liquid, Q is the contact angle of the liquid with the pore surface, D is the pore diameter, R is the gas constant, and T is the absolute test temperature. At the lowest relative vapor pressure, (P/ Po), condensation occurs in the smallest pore. On increase of relative vapor pressure condensation occurs in larger pores.

Features

- Fully automated, simple to use, & very little operator involvement
- Highly reproducible & accurate
- Pressure required is very small.
- Normally liquid nitrogen temperatures are not required
- A wide variety of samples can be investigated
- No toxic material like mercury is used. No health hazard. No disposal related cost.

Operation

The instrument is maintained at the desired temperature. Vapor is introduced in to the sample chamber of known volume. The vapor pressure is monitored until the system comes to equilibrium. From the final pressure, the diameters of pores in which condensation occurs are computed. A small amount of vapor is added to one side of the sample in the sample chamber so as to raise the pressure on that side by about 10 %. The decay of pressure is monitored as a function of time. Gas flow rates through the pores of the sample which do not contain condensed liquid at the maintained pressure of the vapor are computed from the time rate of pressure change. From repeated determination of flow rates at a number of vapor pressures, the flow rate distribution is computed.

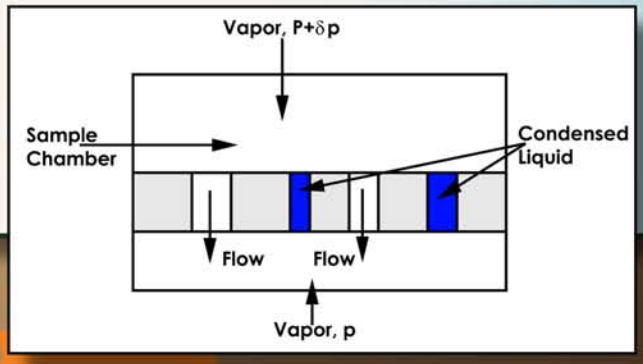

Specifications

- Pore size range: 0.2 – 0.0005 mm
- Pressure: 15 psi
- Accuracy: 0.15% of reading
- Resolution: 1 in 60,000
- Flow rate: As low as 10 -4 cm3/s
- Power: 110/220 VAC, 60/50 HZ

Other Products

Average Fiber Diameter Analyzer
Bubble Point Tester
Capillary Flow Porometer
Capillary Condensation Flow Porometer
Complete Filter Cartridge Analyzer
Clamp-On Porometer
Compression Porometer
Custom Porometer
Cyclic Compression Porometer
Envelope Surface Area Analyzer
Filtration Media Analyzer
High Flow Porometer
Integrity Analyzer
In-Plane Porometer
Microflow Porometer
Nanopore Flow Porometer
QC Porometer
Diffusion Permeameter
Gas Permeameter
Liquid Permeameter
Vapor Permeameter
Water Vapor Transmission Analyzer
Liquid Extrusion Porosimeter
Mercury/Nonmercury Intrusion Porosimeter
Vacuapore
Water Intrusion Porosimeter (Aquapore)
BET Liquisorb
BET Sorptometer
Gas Pycnometer
Mercury Pycnometer

Also Available:
Testing Services
Consulting Services
Short Courses

Buy Rent Lease

Porous Materials, Inc.
20 Dutch Mill Rd, Ithaca, NY 14850 USA
Tel: (607)-257-5544 Toll Free in USA & Canada: 1-800-TALK-PMI
Fax: (607) 257-5639 Email: info@pmiapp.com **WWW.PMIAPP.COM**

06/08

PMI
Porous Materials, Inc.

Permeameters

Gas & Liquid

PMI
Porous Materials, Inc.

Porous Materials, Inc.
20 dutch Mill Road, Ithaca, New York 14580 USA
Toll Free US & Canada: 1-800-TALK-PMI Phone: (607) 257-5544
Fax:(607) 257-5639 Email: info@pmiapp.com

Applications

Permeameters measure:

- Liquid Permeability
- Gas Permeability
- Microflow Permeability
- Diffusion Permeability
- Water Vapor Transmission rate

Permeameters are used in many industries such as chemical, biotech, pharmaceutical, food, beverage, fuel cells, batteries, and pollution control. Materials tested in permeameters include membranes, ceramics, filter media, sintered metal filters, hydrogels, paper, textiles, battery seperators, powder beds, electrodes, foams, sponges, and pen tips.

Principle

Permeameters measure fluid flow rates. The measured flow rates are expressed in liters per minute (LPM) or any other desired unit. Flow rate is often used to compute permeability defined by Darcy's Law:

$(k/\mu) = F / [A(\Delta p / l)]$

The flow at average pressure (F) per unit area (A) of the sample per unit pressure gradient ($\Delta p / l$) across the sample is defined as the ratio of permeability (k) of the samples and viscosity (μ) of the fluid. The cgs unit of permeability is cm^2. Permeability is often given in terms of Darcy, Fraizer, Gurley, or Rayle.

Liquid Permeameter

Instrument

Liquid from a penetrometer tube is forced through the sample. The Differential pressure on the liquid across the sample and the flow rate of the liquid are measured. Pressure is measured by a pressure transducer and liquid flow is measured by the penetrometer.

The fully automated instrument executes tests, acquires data, stores data, and displays data in the desired unit. Windows based operation of the instrument is simple.

Operational Features

- Permeability of a variety of chemicals like phosphoric acid, oil, salt solutions, fat, and body fluids.
- Multiple Sample Chambers for high volume testing
- Measurement at high pressures
- Measurement at elevated temperatures up to 200° C
- Permeability through sample under compression
- Sample chamber that does not require samples to be cut out from the bulk sample

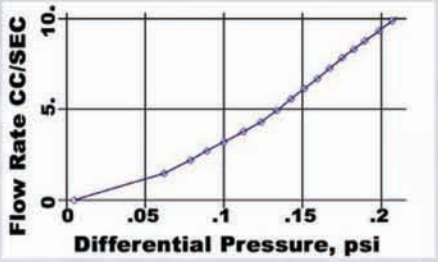

Permeability of KOH solution

Microflow Liquid Permeameters

Instrument

A Microflow liquid permeameter is a liquid permeameter that uses a programmable microbalance to accurately measure a small amount of liquid that may permeate through the sample.

Gas Permeameters

Instrument

Gas under pressure is forced through the sample. The differential pressure and the flow rate of the gas are measured with pressure and flow transducers.

The fully automated instrument executes test, acquires data, stores data, and displays data in the desired unit. Windows based operation of the instrument is simple.

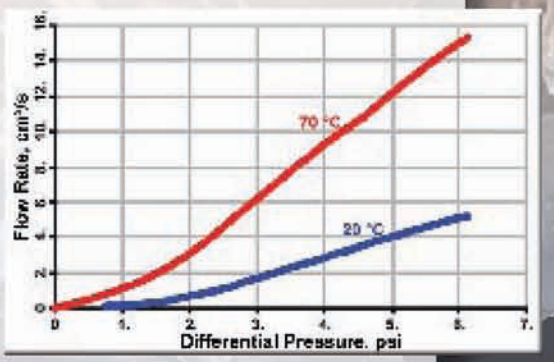

Optional Features

- Permeability of a wide variety of gases
- Multiple sample chamber for high volume testing
- Measurement at high pressures
- Measurement at elevated temperatures
- Sample chamber that does not require samples to be cut out
- Permeability through sample under compression

Microflow Gas Permeameters

Instrument

Gas permeameters cannot measure gas flow rate accurately when the flow rate through the sample is low. Such samples can be examined by microflow permeameters. In these instruments gas is brought to the inlet side of the sample at a known pressure and the increase in pressure on the outlet side is measured. The gas flow rate F at STP is computed from the following relation:

$F = (T_s V/Tps) (dp/dt)$

Where V is volume of the outlet chamber, ps is the standard pressure, (dp/dt) is the rate of pressure increase in the outlet chamber, the test temperature is T, the standard temperature is T_s . The instrument is fully automated. It can have many optional features.

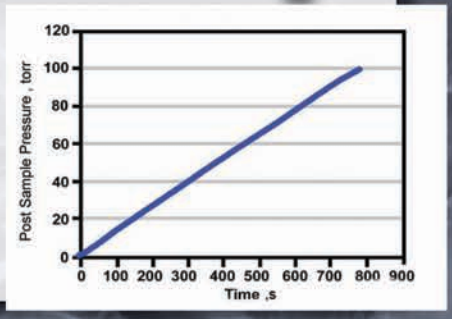

Optional Features

- Microflow permeability can be part of capillary flow porometry
- Measurement at elevated temperatures
- Measurement while sample is under compressive stress
- A wide variety of test gases can be used

Diffusion Permeameter

Instrument

When the gas flow rate through the sample is so low that a microflow permeameter cannot determine the permeability accurately, the diffusion permeameter can be used to measure gas permeability. The sample chamber of the instrument is evacuated first. Gas is maintained at a constant pressure in the inlet side and the increase in pressure in the outlet side is measured. Flow rates are computed as in microflow permeametry.

The instrument is fully automated. Because of evacuation, the instrument is capable of yielding very accurate results and permeability of a variety of gases is measurable. Flow rates as low as 10^{-4} cm^3/s are measurable.

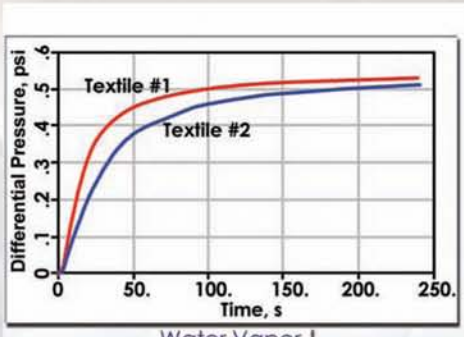

Water Vapor

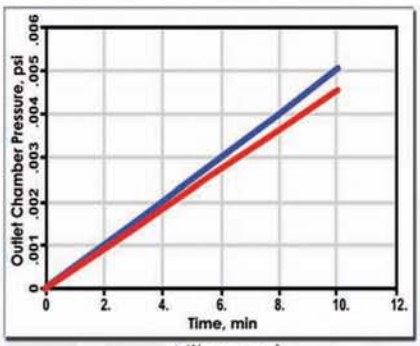

Nitrogen

Water Vapor Transmission Analyzer

Instrument

This instrument uses the dynamic moisture cell (ASTM F2298-03) for measurement of water vapor transmission rate. Transmission across a sample due to imposed humidity gradient, pressure gradient, or both gradients can be measured. The instrument is capable of measuring transmission rate and flow resistance as functions of humidity, pressure, and temperature.

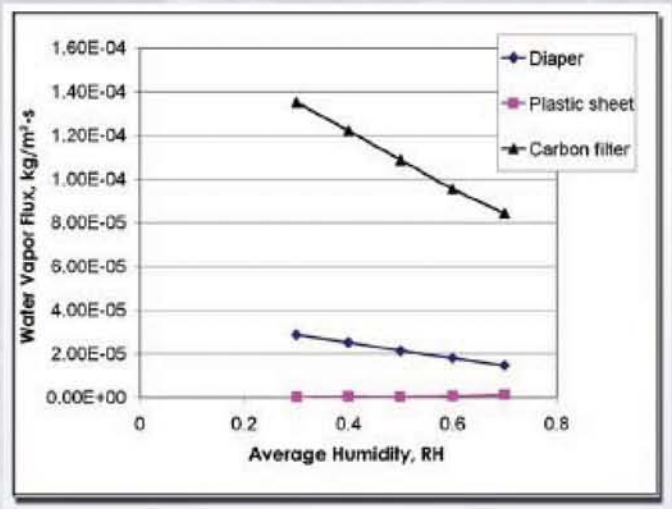

BET SORPTOMETER

Description

PMI's BET Sorptometer accurately measures total surface area (via single and multi-point methods), adsorption and desorption isotherms, mean pore size, pore size distribution, pore volume, and pore structure. PMI's BET Sorptometer can assess a wide variety of samples, including powders and bulk solids, and can analyze both micropores and mesopores. Chemisorption of a wide variety of chemicals is measurable.

Applications

PMI's BET Sorptometer has a multitude of applications in industries worldwide. Industries that utilize the versatile BET Sorptometer include the automotive, battery, and pharmaceutical. Specific applications include the characterization of catalysts in the chemical industry, pulp characterization in the paper industry, and testing of the powder pre-cursors to predict adhesion and final porosity in the powder metallurgy industry.

Applicable industries are:

- Automotive
- Chemical
- Ceramic
- Paper
- Battery Separator
- Fuel Cells
- Filtration
- Pharmaceuticals
- Powder Metallurgy

Principle of the Gas Adsorption Technique

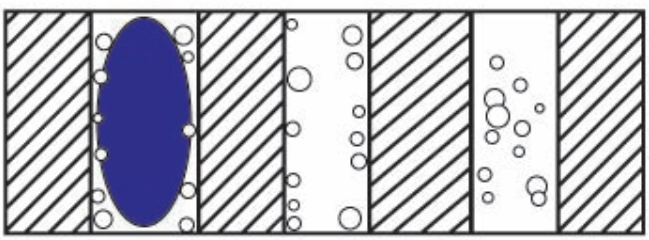

Principle

When a clean surface is exposed to a gas, an adsorbed film forms on the surface. Adsorbed films also form on the surface of pores within a material and vapor can condense in the pores. At a constant temperature, the amount of adsorbed/condensed gas on a surface depends on the pressure of the gas. Measurement of the amount of adsorption/condensation as a function of pressure can give information on the pore structure. The PMI Sorptometers use gas adsorption/condensation to analyze pore characteristics.

Physical Adsorption

Weak van der Waal's type interaction of molecules with a pore surface leads to physical adsorption. The Brunauer, Emmett and Teller (BET) theory of physical adsorption is normally used for analysis of adsorption data to compute surface area.

$$\frac{P}{W(P_o - P)} = \frac{1}{CW_m} + \frac{C-1}{CW_m} X \frac{P}{P_o}$$

where:
W = amount of adsorbed gas
Wm = amount of gas adsorbed in a monolayer
P = gas pressure
Po = equilibrium (saturation) vapor pressure at the test temperature
C = dimensionless constant that depends on the temperature and the gas/solid system

When vapor pressure, P, is low compared with Po ($0.05 < P/Po < 0.3$), the plot of [P/W (Po – P)] versus [P/Po] is linear and the plot yields the magnitudes of C and Wm. The surface area S per unit mass, m, of the sample is computed using the cross–sectional area of the adsorbed gas molecule:

$$S = \frac{W_m N_o \alpha}{m}$$

where:
No = Avogadro's number
a = cross–sectional area of the adsorbed gas molecule
Wm = amount of gas absorbed in moles.

Vapor Condensation

As the relative vapor pressure (P/Po) increases, vapor eventually condenses in the pores utilizing the surface free energy available due to replacement of the solid/vapor interface by solid/liquid interface. The amount of vapor condensed in pores gives the pore volume, and the Kelvin equation gives the pore diameter.

$$\ln\left(\frac{P}{P_o}\right) = - \frac{4 \gamma V \cos \theta}{D R T}$$

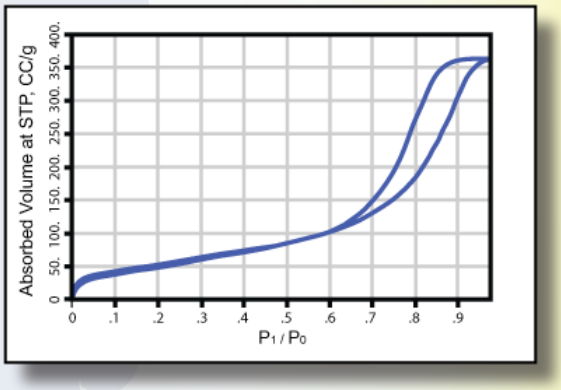

Adsorption and Desorption Isotherms at Liquid N2 temperature

where:
g = surface tension of condensed liquid
V = molar volume of condensed liquid
q = contact angle
D = pore diameter
R = gas constant
T = absolute test temperature

Adsorbed layers of molecules form on the pore walls before condensation fills the pores. Therefore, the actual pore diameters are computed by adding two times the thickness of the adsorbed gas layer to D.

A complete adsorption isotherm is determined by measuring the amount of vapor adsorbed as a function of increasing pressure. A desorption isotherm is determined by measuring the amount of adsorption as a function of deceasing pressure. Based on this technique, characteristics of materials related to adsorption, desorption, surface area and pore volume can be determined.

Chemisorption Chemical reaction between a gas and a surface accompanied by a high heat of adsorption results in chemisorption. Chemisorption data can be analyzed using various theories. Langmuir equation yields:

$$\frac{W}{W_m} = \frac{KP}{1 + KP}$$

where:
W = amount of adsorbed gas
Wm = amount of gas adsorbed in a monolayer
K = equilibrium constant
P = gas pressure

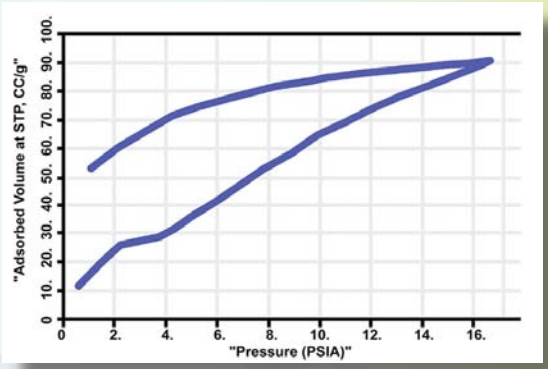

Ammonia Adsorption and Desorption Isotherms at 0 °C

Equipment

The PMI Sorptometer uses volumetric method to compute the amount of gas. The sample chamber is connected through valves to the reference volume, gas supply, & vacuum line. For a test, a weighed sample is placed in the sample chamber. The sample chamber of known volume is heated and evacuated to remove moisture and adsorbed gases. The desired adsorption temperature is then established in the sample chamber using a constant temperature bath, and the chamber is isolated. The reference volume is pressurized with adsorbate gas, and isolated. The pressure of reference volume is measured. The gas is allowed to expand into the sample chamber. After equilibration the gas pressure is measured. The amount of gas adsorbed by the material is calculated by making use of the gas law.

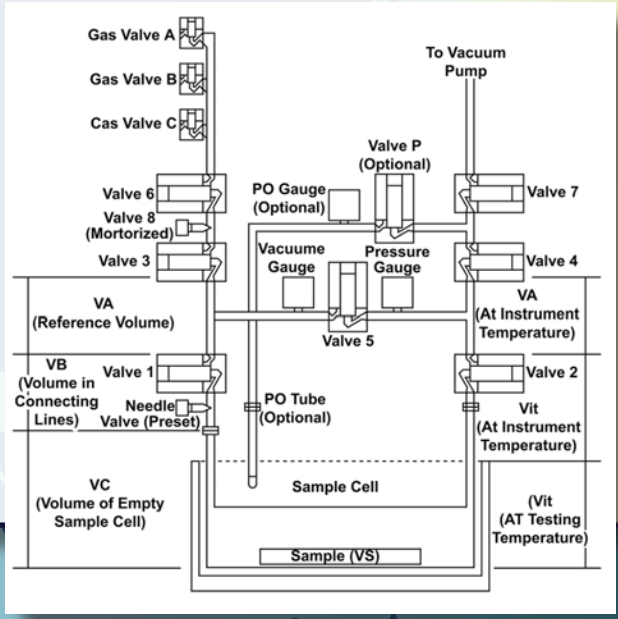

Capabilities

Surface Area:

PMI BET Sorptometers are capable of testing samples with moderate to high surface areas by using nitrogen gas. For samples with very low surface area, a larger amount of sample or krypton gas can be used for greater accuracy. The number and spacing of data points in multipoint surface area measurement are user adjustable.

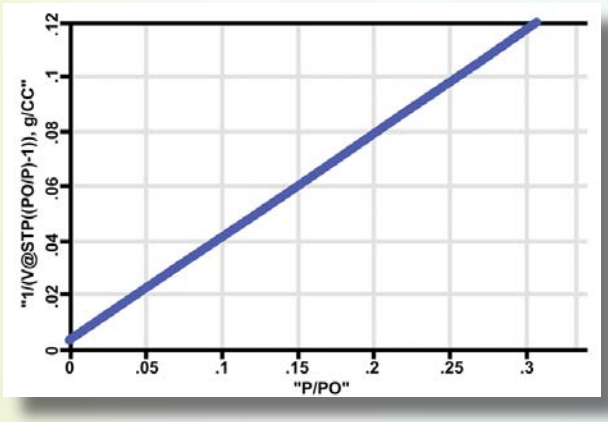

Surface Area Analysis — Nitrogen

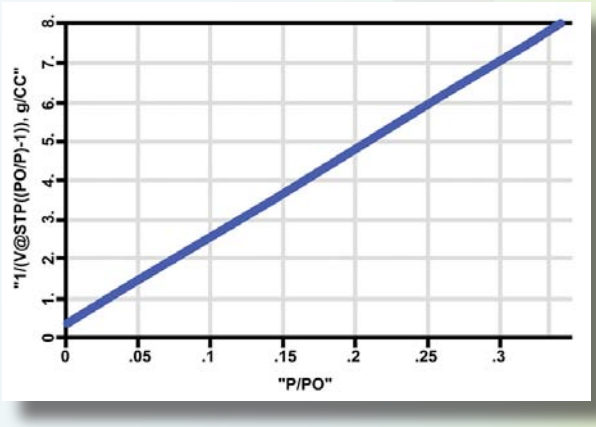

Surface Area Analysis — Krypton

Pore Volume and Pore Diameter

Pore volume, pore diameter and pore volume distribution can be determined accurately by the PMI Sorptometer. The distribution function is such that area under the function in any pore diameter range is the volume of pore in that range.

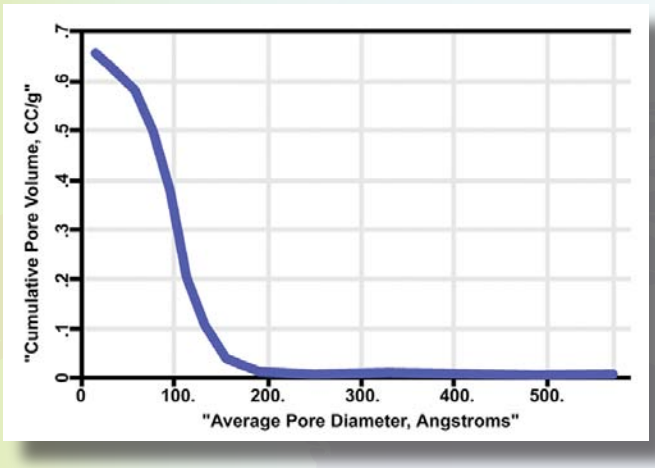

Cumulative Pore Volume

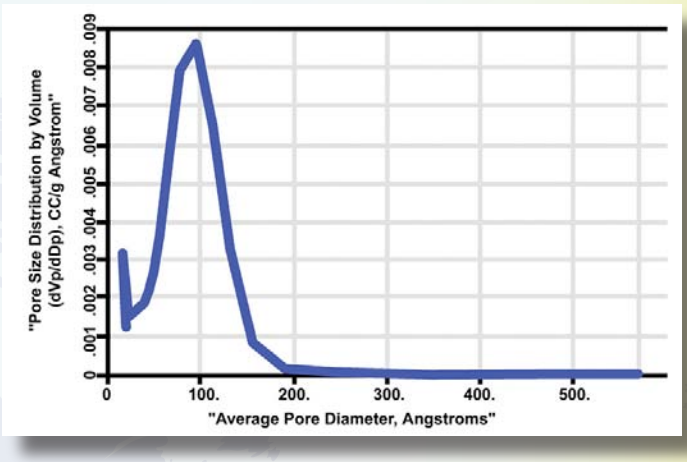

Pore Volume Distribution

Adsorption and Desorption Isotherms

Adsorption and desorption of gasses on samples can be accurately measured using PMI BET sorptometers. The user has independent control over the quantity and spacing of pressures used in both adsorption and desorption testing. Many different kinds of analyses are available to interpret data using the supplied report generation software. Pore size calculation for adsorption and desorption include Pierce, BJK, and DH models. Microporous solids can be analyzed using T–Plot and H–K analysis.

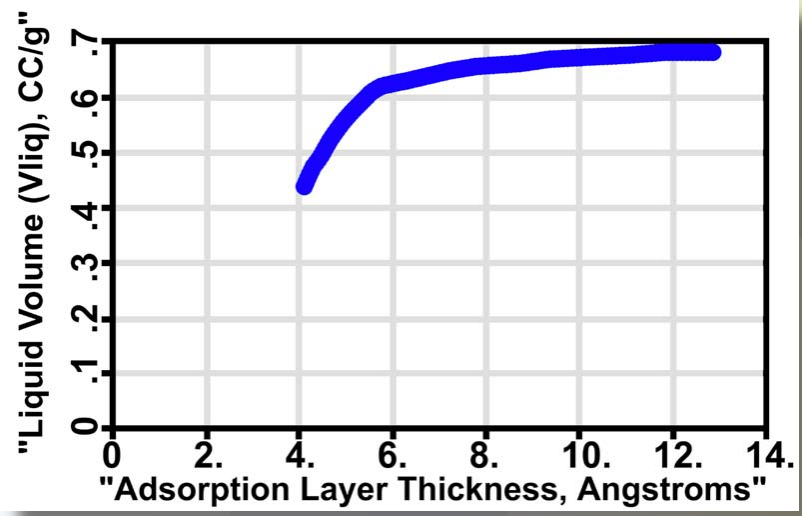

T – Plot Method — Micropore Volume Analysis

Chemisorption:

PMI BET Sorptometers can use specialty gasses like NH3 and H2O for measuring chemisorption. Other gasses can be used by creating additional gas specification files. The user can specify any temperature and pressure of gas, limited only by the capabilities of the instrument and the equilibrium vapor pressure of the gas at the temperature selected.

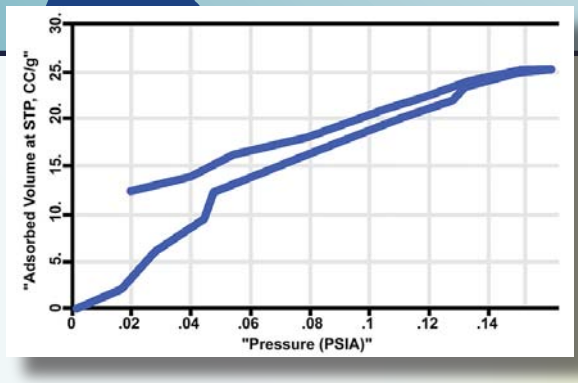

Adsorption and Desorption Isotherms – Water Vapor at 0 °C

Specifications

Surface Area range: 0.01 m2 and higher.
Pore diameter range: Micropore to 2000Å.
Sample volume: Up to 10 cc (others available).
Pressure gauge: 10 torr to 500 psi.
Resolution: 1 part in 20,000
Accuracy: 0.15% of reading
Adsorption temperature: –195.6 deg C (liquid nitrogen) to 300 deg C. (higher temperature available)
Adsorbate: Any noncorrosive gas including N2, H2, CO, CO2, H2O, Kr, Ar.
Degassing system: Heater oven up to 500 deg C (Higher temperatures available).
Degassing and testing performed in–situ.
Power requirements: 110/220 Vac, 50/60 Hz

Unique Features

- Adsorption of chemically active substances like NH3, CO & CO2
- Adsorption of vapors of liquids like water, benzene and alcohol
- Adsorption studies using H2, N2, Ar & Kr
- Adsorption under pressures up to 500 psi
- Adsorption under extra low pressures down to 10 – 5 psi
- Adsorption studies at temperatures up to 300°C & higher
- Use of flow method by QBET series permits fast and reproducible surface area measurements
- Volumetric method employed measures equilibrium amount of adsorbed gas precisely without the possibility of any contamination
- Design features modifiable to satisfy your special requirement
- Any number of user specified data points between specified pressure limits
- Automated calibration routine for different sample chambers
- Continuous status display
- Continuous recording of equilibrium (saturation) pressure
- Data reduction software allows data analysis by many available procedures
  - Surface area: Single point, Multipoint
  - Pore Size: Pierce, NJH and DH models
  - Micropore: t–plot, Langmuir, D–R and H–K model
- Software enables curvefitting and interpolation of data, output to be written in text and Excel files, and multigraph analysis that can analyze up to seven graphs
- Fully automated and minimal operator involvement
- Windows based menu–driven procedure makes test execution, data acquisition, and data reduction very simple
- In–situ outgassing of samples at temperatures up to 800°C
- No need for transfer from outgassing station to test station and increase possibility of contamination
- Multiple sample chambers with provision to use different gases in different sample chambers, and simultaneous testing of multiple samples
- Unique design permits measurement of very low and high surface areas in the same instrument

PMI Analytical Services

PMI has many years of experience in analyzing porous materials using the gas adsorption technique. The analytical services division of PMI is well known for providing timely, accurate and reliable contract testing services. Contact PMI for details.

Models

QBET Series

Units in this series are basic simple instruments dedicated to quick generation of highly reproducible data on surface area using nitrogen or argon. Each unit has one sample chamber. Liquid nitrogen is the only accessory required to perform the test. Various models in this series are capable of measuring single point or multipoint surface area and pore volume. Theses units are least expensive, physically small, robust and require very little maintenance. Model Number: QBET–G–X–Y–A

CBET Series

Instruments in this series are volumetric compact units, but the capabilities are much better than those of the QBET series. These instruments can measure surface area, adsorption and desorption isotherms, pore volume and pore volume distribution using nitrogen, argon and krypton. The results are reproducible and accurate. Models in this series are inexpensive, and robust. These models require very little maintenance. Model Number: CBET–G–D–Y–A

ABET Series

Models in this series are the most advanced instruments in which many novel and advanced designs are incorporated. These instruments are capable of measuring very low adsorption, chemical adsorption and water vapor adsorption. The results are highly accurate and reproducible. Multiple sample chambers permit testing of as many as six samples at a time. A variety of gases may be used. The advanced series provides many options to the user. Model Number: ABET–G–D–Y–A–L–C–W

Brief Descriptions of Selected Models

Model: QBET–N–V–1–A
This fully automated sorptometer is a single–chamber instrument that can determine single point surface area, multipoint surface area and pore volume using nitrogen as the adsorption gas. The instrument is small, robust and inexpensive. It requires very little maintenance. The sorptometer is ideal for applications such as quality control requiring rapid generation of reproducible data.

Model: CBET–N / Kr/Ar–D–2–A
This table top compact model can measure single point surface area, multipoint surface area and pore volume using N2, Kr or Ar as the adsorption gas. The instrument is fully automated and has two sample chambers. Two samples can be tested simultaneously. This option gives the opportunity to compare samples with the standard. The model is also robust and inexpensive.

Model: ABET–G–D–6–A–L–C–W
This is a sophisticated unit with many capabilities. It uses gases like N2, Ar, Kr, H2 and CO2 for adsorption and measures single point surface area and pore volume distribution. Chemical adsorption of substances like ammonia, alcohol and benzene is measurable. The results are accurate and reproducible. The instrument is fully automated and requires very little operator involvement. The six sample chambers of the instrument permit simultaneous testing of six samples. The sorptometers are ideal for determination of a variety of physical and chemical characteristics.

Symbols

A = fully automated
C = chemical adsorption of many chemical species
D = surface area, pore volume and pore distribution
G = adsorption gas that could be N2, Ar, Kr, H2 or others
L = very low adsorption pressure
V = single point and multipoint surface area and pore volume
W = water vapor adsorption capability
X = type of test
Y = number of sample chambers

Highlights of PMI BET Sorptometer Models

Features	QBET SERIES	CBET SERIES	ABET SERIES
Principle	Flow	Volumetric	Volumetric
Design:	Simple	Moderately Complex	Complex
Gases	N_2/Ar	N_2/Ar/Kr	N_2/Ar/Kr/CO_2/ H_2/NH_3/Others
Liquid N_2 Bath:	Container with cover	Container with Cu–block and cover	**Refill system**
Measurable Properties:	Single point and multipoint surface area. Pore volume	Single point & mulitipoint surface area. Pore volume. Pore distribution. Desorption.	Single point & multipoint surface area. Pore volume. Pore distribution. Desorption. Very low adsorption. Chemisorption. Water vapor adsorption.
Reliability:	Highly reproducible	Highly reproducible and accurate	Highly reproducible and very accurate
Duration of Test:	Short	Moderate	Long
Size:	Small	Table Top	Floor Model
Maintenance:	Very Little	Very Little	Regular
Cost:	Low	Medium	High

New Sorptometers

PVT Apparatus

Other Products

Average Fiber Diameter Analyzer
Bubble Point Tester
Capillary Flow Porometer
Capillary Condensation Flow Porometer
Complete Filter Cartridge Analyzer
Clamp-On Porometer
Compression Porometer
Custom Porometer
Cyclic Compression Porometer
Envelope Surface Area Analyzer
Filtration Media Analyzer
High Flow Porometer
Integrity Analyzer
In-Plane Porometer
Microflow Porometer
Nanopore Flow Porometer
QC Porometer
Diffusion Permeameter
Gas Permeameter
Liquid Permeameter
Vapor Permeameter
Water Vapor Transmission Analyzer
Liquid Extrusion Porosimeter
Mercury/Nonmercury Intrusion Porosimeter
Vacuapore
Water Intrusion Porosimeter (Aquapore)
BET Liquisorb
BET Sorptometer
Gas Pycnometer
Mercury Pycnometer

Also Available:
Testing Services
Consulting Services
Short Courses

Buy Rent Lease

Porous Materials, Inc.
20 Dutch Mill Rd, Ithaca, NY 14850 USA
Tel: (607)-257-5544 Toll Free in USA & Canada: 1-800-TALK-PMI
Fax: (607) 257-5639 Email: info@pmiapp.com **WWW.PMIAPP.COM**

PMI Porous Materials, Inc.

Hydrophobic Pore Structure Characteristics of Fuel Cell Components Using Vacuapore

Dr. Akshaya Jena and Dr. Krishna Gupta

Porous Materials, Inc.

20 Dutch Mill Road, Ithaca, NY 14850

Abstract: *Important pore structure characteristics of hydrophobic fuel cell components such as Pore volume, pore diameter, pore volume distribution, effects of compressive stress on pore structure characteristics and in-plane pore structure are not measurable by available nonwetting liquid intrusion techniques. A novel Vacuapore technique has non of the disadvantages of the available techniques and can measure all the characteristics.*

Keywords: Pore Volume; Pore Diameter; Pore Distribution; Hydrophobic Pores; Effects of Compressive Stress; In-Plane Pore Structure.

Characterization Requirements

Structural characteristics of hydrophobic pores of fuel cell components determine water management, transport of reactants, reaction rates, and flow rates of reaction products. Fuel cell components are also subjected to considerable compressive stress, which influences the pore structure characteristics [1]. The primary relevant pore structure characteristics of hydrophobic materials used in fuel cell applications are pore volume, pore diameter, pore volume distribution, in-plane pore structure, and effects of compressive stress on pore structure. It is important to be able to measure these pore structure characteristics so that optimum and efficient fuel cells may be designed.

The Technique

Principle: For measurement of pore volume, the sample is surrounded by a nonwetting liquid. Nonwetting liquids can not spontaneously enter the pores of the sample because the sample-nonwetting liquid surface free energy is greater that the sample-vapor surface free energy. Application of pressure on the nonwetting liquid results in the intrusion of the nonwetting liquid in to the pores of the sample. The measured decrease in volume of the nonwetting liquid is the pore volume. The measured differential pressure on the nonwetting liquid yields the pore diameter [2].

$$D = - 4 \gamma \cos \theta /(p-p_g) \qquad (1)$$

where D is pore diameter, γ is the surface tension of the nonwetting liquid, θ is the contact angle of the nonwetting liquid with the sample, p is the pressure on the nonwetting liquid, p_g is the pressure of trapped gas in the pore, and $(p-p_g)$ is the differential pressure on the wetting liquid.

*Limitations of Available Characterization Techniq*ues: Mercury intrusion porosimetry has been used to characterize pore structure of hydrophobic materials. In this technique, the sample is evacuated and mercury is employed as the nonwetting liquid. Equation 1 is used for computation taking p_g to be zero. This technique requires very high intrusion pressures. It is not possible to accurately apply small intrusion pressures for characterization of large pores, which can not be accurately measured. Also, large intrusion pressures compress small pores. Therefore, diameter s and volumes of small pores are not accurately measurable and volume of large pores becomes higher. This technique can not measure the in-plane pore structure and the effects of compressive stress on pore structure.

Water Intrusion Porosimetry or Aquapore technique has also been used to measure pore volume of hydrophobic pores. In this technique, water, which in nonwetting to hydrophobic materials, is used as the intrusion liquid. This technique has the advantage of using very low intrusion pressures. Thus, the undesirable effects of high intrusion pressure are avoided. However, the sample is not evacuated. Therefore, the gas which remains trapped in pores prevents measurement of pore volume and diameter of large pores, which require small intrusion pressures. This technique can not measure the in-plane pore structure and the effects of compressive stress on pore structure.

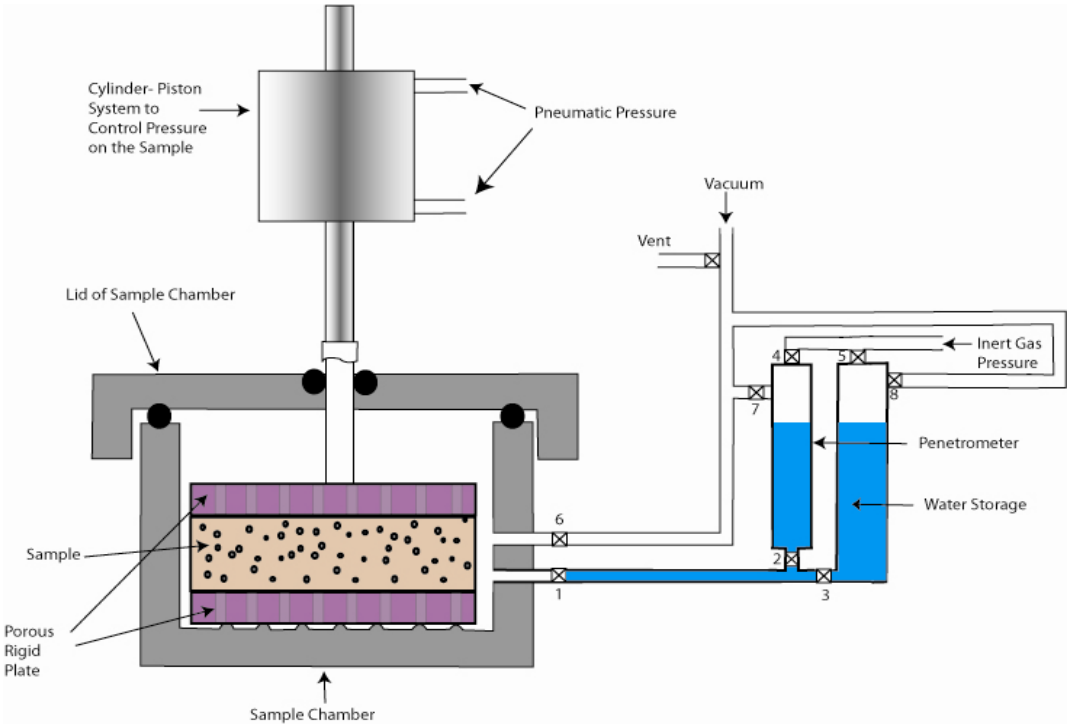

Figure 1. Important features of the Vacuapore

The Novel Vacuapore Technique

In the novel vacuapore technique, water is used as the nonwetting liquid for characterization of hydrophobic materials, so that the intrusion pressure is low and the drawbacks associated with the use of high intrusion pressures are avoided. The sample is evacuated so that the limitations due to air trapped in the pores are eliminated. A novel instrument design is incorporated so that it becomes possible to test effects of compressive stress on pore structure and to measure the in-plane pore structure.

The Instrument: The layout of the instrument is shown in Figure 1. The sample is held between two rigid plates with large holes. The bottom plate is placed on corrugated bottom of the sample chamber. The top plate is connected to a rod that passes through a pressure tight seal in the lid and is linked to a piston–cylinder device pneumatically operated for accurately applying controlled compressive stress on the sample. This arrangement permits sample to be kept under desired compressive stress of zero or higher and intrusion of water in to pores of the sample from all sides. The sample chamber is in communication with a penetrometer through valves 1 and 2. On application of pressure on water in the penetrometer, water intrudes in to pores of the sample. The decrease in the volume of water in the penetrometer is the pore volume. For measuring the change in the volume of water, the change in the position of a magnet floating on water in the penetrometer is measured. The penetrometer is filled with water from a water reservoir connected to the penetrometer through valve-3. The penetrometer and water reservoir are connected through valve-4 and valve-5 respectively to a gas line capable of supplying an inert gas at an adjustable controlled pressure for pressurization of water. The sample chamber containing the sample is in communication with a vacuum line through valve-6. The vacuum line is also in communication with the penetrometer through valve-7, and to the storage vessel through valve-8 for evacuation above the water level. A vent valve is provided in the vacuum line. This unique design permits evacuation of sample chamber and the space above water in the penetrometer to be performed independently and separately so as to permit elimination of problems due to trapped air in the system. In order to create small sub-atmospheric pressures, a special device called vacuum regulator is used for controlled release of vacuum and creation of the desired sub-atmospheric pressures on water.

Procedure: The sample is loaded in the clean sample chamber. The sample chamber cap is sealed. Air pressure is used to operate the piston-cylinder device to apply desired compressive stress on the sample. The sample chamber is evacuated. The penetrometer and water storage are also evacuated. Water is

allowed to enter the sample chamber. The pressure on water is increased. The pressure on water and the decrease in volume of water in the penetrometter due to intrusion in pores are measured.

Application

Low Test Pressure for Intrusion: Figure 2 shows the change of cumulative pore volume with increase in differential pressure. The results from a mercury intrusion porosimeter are also shown in the figure for comparison with the results of the water intrusion test. The pressures for water intrusion are much less.
Through Pore and Blind Pore Volume: The pore volume shown in Figure 2 is the volume of through and blind pores because water intrudes both pores. Because of evacuation, the air trapped above water in the sample chamber is negligible and any increase in intrusion volume because of compression of the trapped air at higher pressures is also negligible. The initial intrusion pressures are close to the vapor pressure 0.3 psi of water at the test temperature of 18˚C. The intrusion pressure is increased rapidly the vapor may not get time to condense. Therefore, even at intrusion pressure as low as 1 psi, at the most only a small part of the pore will be undetected because of vapor contained in the pore.

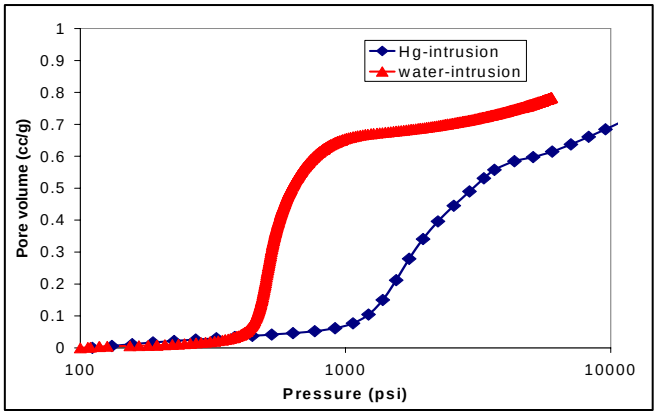

Figure 2. Change of pore volume with intrusion pressure for water intrusion and mercury intrusion

Through Pore and Blind Pore Diameter: The pore diameter is computed using Equation 1 (Figure 3). The pressure in the pore, p_g, used in this equation will be equal to or less than the small pressure of gas left in the pore after evacuation because part of the air left in the pores will be absorbed by the intruding evacuated unsaturated water. Because of short test duration, water is unlikely to have sufficient time to evaporate and maintain its equilibrium vapor pressure in pores. If water is able to main its equilibrium vapor pressure of 0.3 psi during the normally short test, the pressure of air in the pore, p_g, will be 0.3 psi. This small pressure is mostly negligible and pore diameters are accurately measured. When intrusion pressure is increased, diameters of large pores may not be measurable if the vapor does not condense.

Through Pore and Blind Pore Volume Distribution: The through pore and blind pore volume distribution is given in terms of the distribution function, $f_v(\log D)$ in terms of cumulative pore volume, V.

$$fv(\log D) = -(dV / d \log D) \qquad (2)$$

The area under the distribution function in any pore diameter range is the volume of pores in that range **(Figure 4).**

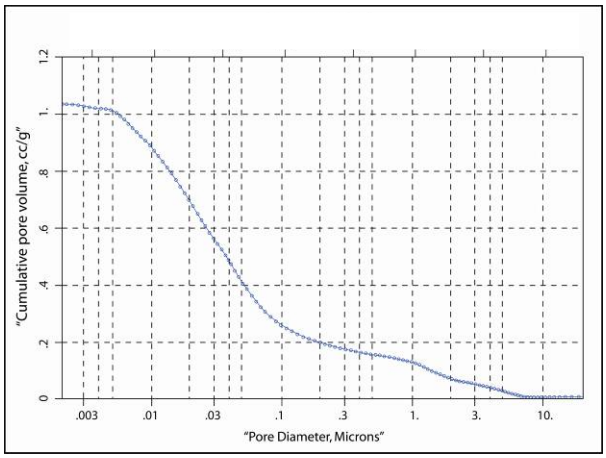

Figure 3. Change of cumulative pore volume with pore diameter

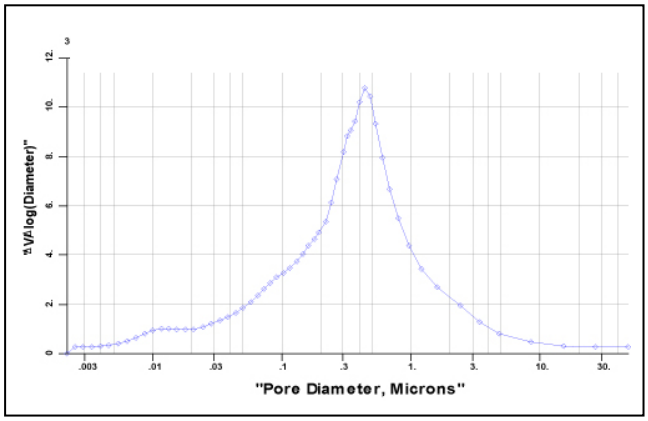

Figure 4. Pore volume distribution

In-Plane Pore Structure: The sample is sandwiched between two rigid nonporous plates having no holes. Therefore, water radially intrudes the pores in the sample in the x-y plane. The pore structure of radial pores are evaluated.

Effects of Compressive Stress on Pore Structure: Sample is put under desired compressive stress and pore structure is characterized. Thus, the influence of compressive stress on pore structure is evaluated.

Summary & Conclusions

A novel technique , Vacuapore, has been described. It can measure pore volume, pore volume distribution, in-plane pore structure, and pore structure of the in-plane. Results have been presented to illustrate the application

References

1. Lee, W-K, W. V. Zee, A. K. Jena, and K. Gupta, "Characterization of Permeability Changes and Hydrophobic Nature of GDL and Their Correlation with PMFC Performance", *Proceedings Fuel Cell Seminar*, San Antinio, Texas, 2004.

2. Jena, Akshaya, and Krishna Gupta, "Characterization of Pore Structure of Filtration Media", *Fluid/Particle Separation Journal*, vol.14. no. 3, pp.227-241, 2002.

Characterization of Porosity of Electrodes and Separators in Fuel Cell Industry

Akshaya Jena and Krishna Gupta
Porous Materials Inc
83 Brown Road, Ithaca, NY 14850

Abstract

Pore size, pore structure, permeability, and surface area are some of the important characteristics that need to be measured for designing efficient electrodes and separators as well as evaluating their performance. For such measurements, we used the PMI Capillary Flow Porometer. The pores of the sample were filled with a wetting liquid and then pressurized air was applied on one side of the sample to remove the liquid from the pores and increase the flow rate of the gas. The flow rate through wet and dry samples, measured as a function of gas pressure, yielded the pertinent data. The data were highly reproducible and accurate. This technique of pore characterization has a number of advantages over other techniques.

INTRODUCTION

Electrodes and battery separators are critical components of fuel cells and batteries. In many designs, the gaseous fuel passes through the porous electrodes and reacts with other components in the electrolyte at the surface of the electrode. The pore surface area controls the rate of reaction. The resistance to flow is governed by the pore size distribution of the electrode and the permeability of the electrode. The battery separator separates the electrodes. The pores of the separator provide sufficient permeability for liquid to flow, and the largest pore of the separator allows only selected components of the electrolyte to pass through. Therefore, the pore structure of battery separators and electrodes needs to be monitored for efficient design and operation of these components. In this investigation, we used a capillary flow porometer to measure the largest pore size, pore size distribution, permeability, and surface area of electrode and separator materials.

EXPERIMENTAL PROCEDURE

In this technique a sample of the material is soaked in a liquid that fills the pores in the sample spontaneously. The sample is placed in the sample chamber (Figure 1) and is maintained at the desired temperature. Pressure of air or some other suitable gas on one side of the sample is gradually increased. The chamber is designed so that the gas passes either parallel to the thickness of the sample (Through-plane flow) or parallel to the plane of the sample (In-plane flow). The in-plane and the through-plane pore characteristics are separately determined by using the appropriate sample chamber.

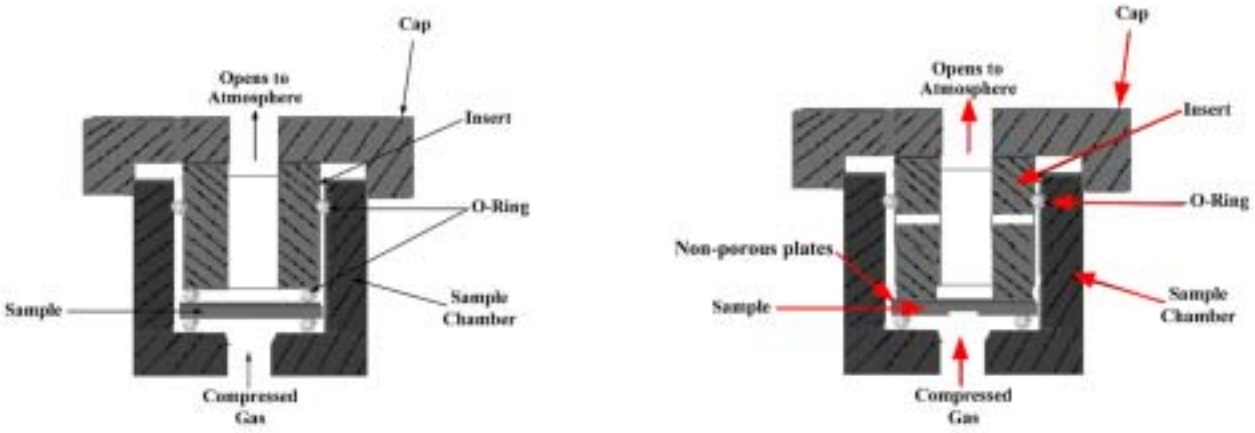

(a) Through plane (b) In-plane

Figure 1. Sample chamber

Initially the gas does not flow through the sample because the liquid in the pores prevents flow. When the pressure is sufficient, liquid from the largest pore is emptied and the flow of the gas starts. With increase in pressure, smaller pores are emptied and the flow of gas increases. The PMI Capillary Flow Porometer was used in this study. It measured pressure and flow rate accurately. The data acquisition and management were carried out through windows based software [1,2]. The porometer generated highly reproducible data [3]. The pressure of gas and the corresponding flow rate were accurately measured using wet as well as dry samples. From these data, the largest pore size, pore size distribution, permeability, and surface area were calculated. A typical plot of flow rate as a function of

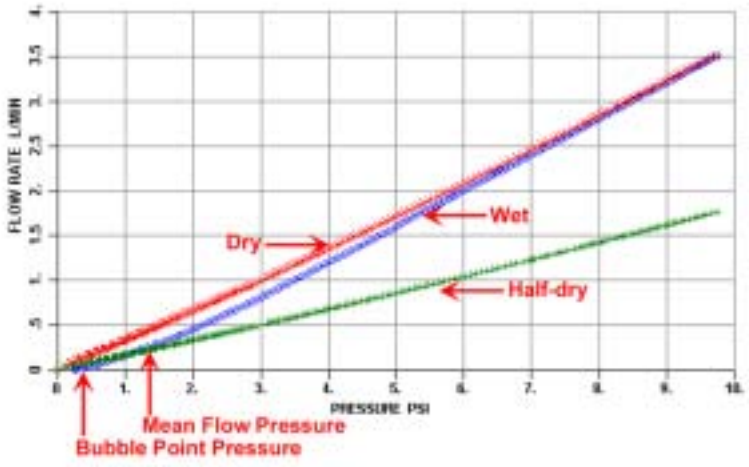

pressure is shown in Figure 2.

Figure 2. Variation of flow rate with differential pressure for battery separator #1.

ANALYSIS

Filling the pores of a sample with a liquid involves creation of solid/liquid interfaces in place of solid/gas interfaces. If the solid/gas interfacial free energy is higher than the

solid/liquid interfacial free energy, the process of filling the pores with liquid will decrease the free energy of the system and thus, make the process spontaneous. The liquid that fills the pores spontaneously is known as a wetting liquid. When gas displaces liquid inside pores, the solid/gas interface replaces the solid/liquid interface, and the free energy of the system increases (Figure 3).

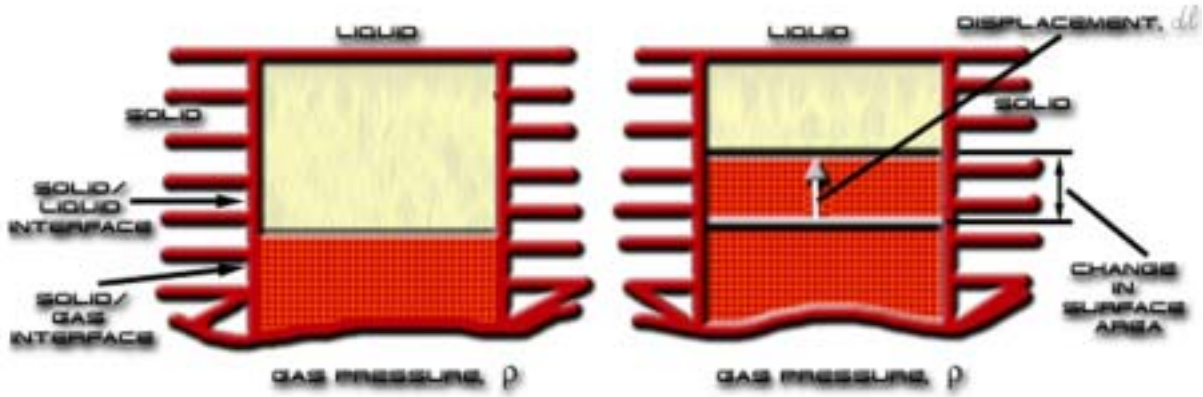

Figure 3. Displacement of liquid by gas.

In order to displace the liquid inside the pore, the gas does work on the system to compensate for the increase in the interfacial free energy [4]. The work done by the gas is represented by pdV, where p is the gas pressure at the inlet relative to that at the outlet and dV is the infinitesimal increase in volume of the gas inside the pore. The work done by the gas must be equal to the increase in the interfacial free energy. The displacement of the gas inside an opening changes the surface areas (Figure 4).

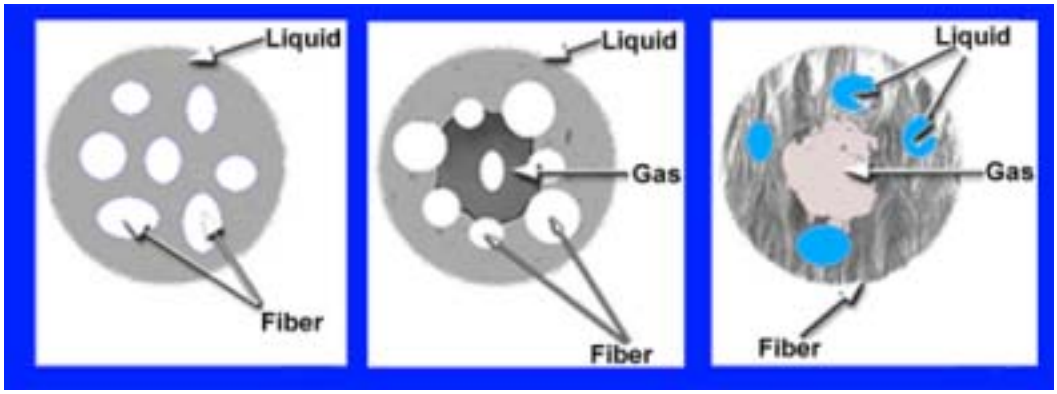

Figure 4. Increase in surface area. (a) Fibrous material containing liquid. (b) Opening in fibrous material filled with gas. (c) Opening in non-fibrous material filled with gas.

Let the increases in the solid/gas and liquid/gas surface areas due to infinitesimal increase in the volume of the gas, be $dS_{s/g}$ and $dS_{l/g}$ respectively. Then [5]:

$$p\,dV = (\gamma_{s/g} - \gamma_{s/l})\,dS_{s/g} + \gamma_{l/g}\,dS_{l/g} \qquad (1)$$

where:
$\gamma_{l/g}$ = liquid/gas interfacial free energy
$\gamma_{s/g}$ = solid/gas interfacial free energy
$\gamma_{s/l}$ = solid/liquid interfacial free energy.

Equation 1 may be written as:

$$p = \gamma_{l/g}\, \beta\, (dS_{s/g}/dV)\, [\, 1 + (f/\beta)] \qquad (2)$$

where, $\beta = [(\gamma_{s/g} - \gamma_{s/l}) / \gamma_{l/g}]$, and $f = (dS_{l/g} / dS_{s/g})$.

Consideration of equilibrium between the three interfacial free energies (Figure 5) shows [6] that $\cos\theta = (\gamma_{s/g} - \gamma_{s/l}) / \gamma_{l/g}$, where θ is the contact angle, and $\beta = \cos\theta$. For wetting liquids, normally $\beta \sim 1$. However, if the interfacial free energies are such that equilibrium is not possible (Figure 4), then β is greater than 1 [3].

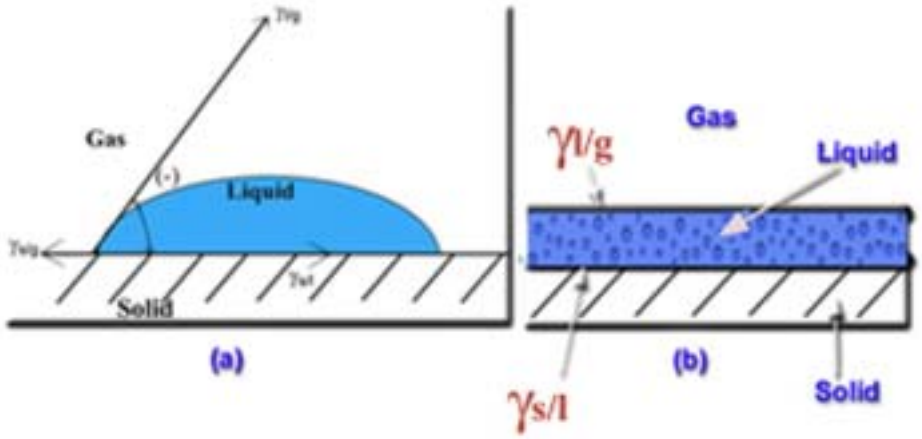

(a) $0 \le [(\gamma_{s/g} - \gamma_{s/l}) / \gamma_{l/g}] \le 1$. Equilibrium possible.

(b) $[(\gamma_{s/g} - \gamma_{s/l}) / \gamma_{l/g}] > 1$. Equilibrium not possible.

Figure 5. Equilibrium between surface tensions

It has been shown that β in Equation 2 is equal to 1 for wetting liquids with small values of interfacial free energy [3]. The magnitude of f in Equation 2 is determined by the structure of the path of gas flow. Paths are created by interconnected voids present in the filter. Normally, samples are either fibrous or non-fibrous. Cross-sections of typical paths in fibrous and non-fibrous materials are illustrated in Figure 4. The interfacial area of fibrous materials is almost entirely due to the outer surfaces of fibers, and the magnitude of the term $(dS_{l/g} / dS_{s/g})$ is negligible. In case of non-fibrous materials, the term $(dS_{l/g} / dS_{s/g})$ is zero. Consequently, for both non-fibrous and fibrous materials, Equation 2 reduces to:

$$p = \gamma_{l/g} \cos\theta \ (dS_{s/g}/dV) \quad (3)$$

The magnitude of $(dS_{s/g}/dV)$ in this equation is a function of the location along the path of the gas. For a displacement dl, of the gas/liquid interface (Figure 3) at a location in a pore of circular cross-section of radius, r, $(dS/dV) = (2\pi r\, dl / \pi r^2\, dl) = (2/r)$. This example illustrates the fact that (dS/dV) increases with decrease in the size of cross-section along the length of the pore. Because the pore size changes along the length of a pore, the pressure required to displace the liquid in the pore is different at different locations and has the maximum value at the pore's most constricted location. Therefore, the pressure required to clear a pore of the wetting liquid is determined by the maximum value of (dS/dV) at the most constricted part of the pore. Thus, pressure is a measure of the size of the pore at its most constricted location. The arrows in Figure 6 illustrate the locations of the most constricted part of each pore.

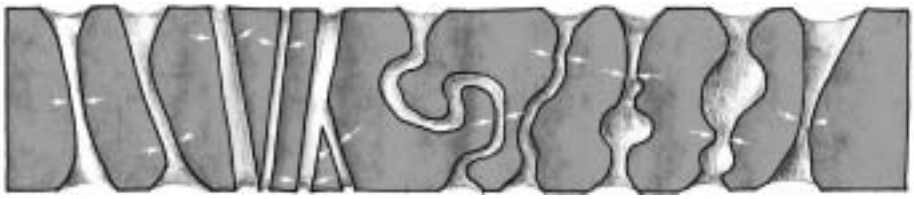

Figure 6. Sketch illustrating a range of pore sizes and the most constricted pore sizes

Equation 3 shows that pressure is a measure of $(dS_{s/g}/dV)$ of the pore at its most constricted part. However, $(dS_{s/g}/dV)$ is not a convenient quantity to use as the measure of pore size. For a circular cross-section of diameter D:

$$(dS_{s/g}/dV) = 4/D \quad (4)$$

However, in case of non-circular cross-sections (Figure 7), $(dS_{s/g}/dV)$ cannot be specified in any simple way.

Figure 7. Examples of pore cross-sections

We define the diameter of a non-circular cross-section as the diameter of a circular opening that has a $(dS_{s/g}/dV)$ value the same as that of the pore cross-section. Pore diameters defined in this manner are calculated using the following relation derived from Equations 3 and 4:

$$D = 4 \gamma_{l/g} \cos \theta / p \quad (5)$$

Thus, if p is the measured value of pressure that is required to empty a pore, D calculated from Equation 5 gives the diameter of an opening of circular cross-section whose ($dS_{s/g}/dV$) value is the same as that of the actual pore at its most constricted point.

RESULTS AND DISCUSSION

Pore diameter

The data obtained from the porometer (Figure 2) can be used to calculate a number of characteristics of the pore structure of the sample. The pressure at which the flow of the gas begins (The bubble point pressure), corresponds to the pressure required to empty the largest pore. This pressure is used to calculate the diameter of the largest pore in the sample. The half-dry curve in the figure gives half of the flow rate through the dry sample at the same pressure. The intersection of the wet and the half-dry curves give the mean flow pressure, which is used to calculate the mean flow pore diameter. The mean flow pore diameter tells us that half of the flow through a dry sample is through pores having diameter greater than the mean flow pore diameter. The largest pore diameter and the mean flow pore diameters of two battery separators and an electrode are listed in Table 1.

Table 1. Largest pore diameter and mean flow diameter

Sample	Largest diameter, μm	Mean flow diameter, μm
Battery separator		
#1	25.5247	6.6292
#2	36.7299	26.5967
Electrode	46.6762	14.1186

Flow distribution

We use a model of the porous material in which the sample thickness is *l*, the pores are cylindrical of length *l*, and the pore diameter is proportional to the measured constricted pore diameter. Assuming the flow to be viscous [7], and expressing the flow rate F, in volume at STP per unit time, we express the flow rate through the porous sample in the following form:

$$F = [\pi\beta/ (128 \mu l 2p_s)] [p_i+p_o] [\sum_i N_i D_i^4][p_i- p_o] \quad (6)$$

where, μ is the viscosity of gas, p_s is the standard pressure, p_i is the inlet pressure, p_o is the outlet pressure, N_i is the number of pores of diameter D_i. The equation shows that the variables are separable and the flow rate may be expressed as the product of two functions; f(p) and g(D,N, …). Thus:

$$F = f(p).g(D,N, \ldots) \tag{7}$$

The ratio of $F_{w,i}$ and $F_{d,i}$, which are the flow rates of wet and dry samples respectively at the same pressure p_j, becomes:

$$(F_{w,j} / F_{d,j}) = [g(D,N, \ldots)]_{w,j} / [g(D,N, \ldots)]_{d,j} \tag{8}$$

Thus, $(F_{w,j} / F_{d,j})$ is independent of pressure at which it is measured. We define F(D) as the flow distribution function. Hence:

$$(F_{w,j} / F_{d,j}) = \int^{Dj} F(D)dD \tag{9}$$

$$\begin{aligned} F(D) &= - d(F_{w,j} / F_{d,j}) / dD \\ &= - [(F_{w,j+1}/F_{d,j+1}) - (F_{wj} /F_{d,j})] / [D_{j+1} - D_j] \end{aligned} \tag{10}$$

The fact that the flow rate increases with decrease in pore diameter, is incorporated in Equation10 by including the negative sign in the equation. The flow distributions, calculated for the battery separator and the electrode are presented in Figures 8 and 9.

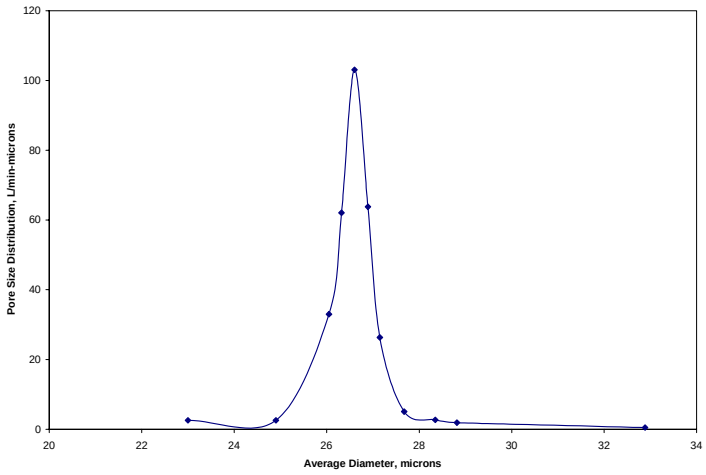

Figure 8 Flow distribution of battery separator #2.

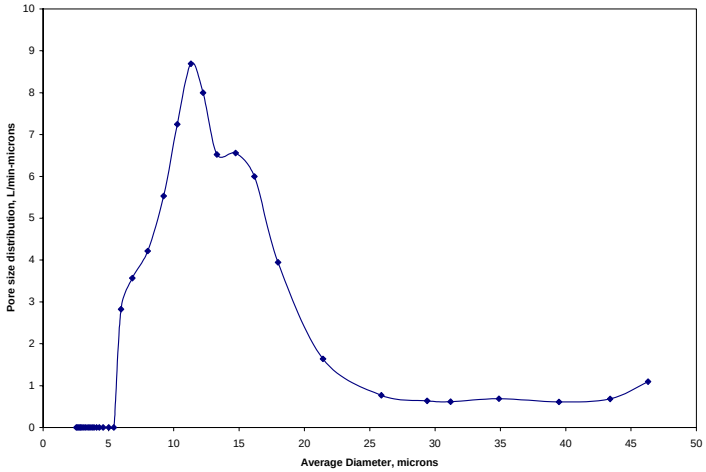

Figure 9. Flow distribution of electrode.

Permeability

Gas permeability k, through a sample is related to the flow rate through the following relation:

$$F = k\,(A / 2\mu l\, p_s)\,(p_i + p_o)[\,p_i - p_o] \qquad (11)$$

where A is the surface area of the sample. Therefore, gas permeability is directly obtained from the dry curve. Permeabilities of the electrode and the battery separator #1, calculated from the dry curves are listed in Table 2 for three differential pressures.

Table 2 Air permeability of electrode and battery separator.

Differential pressure psi	Permeability of battery separator #1, $\times 10^3$ Darcy	Permeability of electrode, $\times 10^3$ Darcy
0.535	8.412	800.4
1.13	7.852	784.6
3.33	7.367	732.1

It is clear from the table that permeability depends upon the average pressure at which the measurement is made. The effect of pressure could be appreciable depending upon pore diameter, porosity, and tortuosity.

Liquid permeability of electrodes and battery separators can also be determined in the same instrument by measuring the liquid flow rate.

Envelope surface area

The envelope surface area S, of all the through pores per unit weight of the sample of porosity P, and true density ρ, is given by:

$$S = [P/(1-P)\rho] \sqrt{[P(p_i - p_o) / (f\, l\, \mu\, \nu)]} \qquad (12)$$

where ν is the approach velocity and f is a constant that has a value of 5 for most materials. Porometer measures the approach velocity. The envelope surface area is calculated by combining the approach velocity measured in the porometer with values of porosity and true density measured separately by pycnometry.

Advantages of capillary flow porometry

Flow poprometry has a number of advantages over other techniques such as porosimetry and nitrogen adsorption.

(1) No toxic material is used in the test.
(2) Very high pressures, where the sample may get damaged or the pore structure may get distorted, are not used for the test.
(3) The test is normally performed at room temperature rather than the liquid nitrogen temperature
(4) The test is non-destructive. The sample is not damaged or contaminated. It is reusable.
(5) The test does not require much preparation time and takes only a few minutes to be executed. This results in the saving of a lot of the operator's valuable time.
(6) The fully automated instrument interfaces with windows based software for data acquisition and management. Thus, highly reproducible and objective data are obtained.
(7) Only the through pores are tested. Therefore, this technique is more appropriate for characterizing battery separators and electrodes.

CONCLUSIONS

1. Flow rates of air through wet and dry samples of an electrode and two battery separators were measured in the PMI Capillary Flow Porometer.
2. Using these data it was possible to calculate the largest pore size, the mean flow pore size, the distribution function of fractional flow for pores of various sizes, and permeability. It was also shown that the surface area of pores can be calculated if the porosity and the true density are measured separately using pycnometry.
3. The results were highly reproducible.
4. The technique of flow porometry that was used in this investigation has a number

advantages over other techniques. Flow porometry does not use high pressures or very low temperatures. No toxic mater is involved in the test. The actual test takes only a few minutes and saves a lot of the operator's time.

REFERENCES

1. R.V. Webber, Recent Advances in Automated High Accuracy Bubble Point Measurement, Filtration News, January/February, pp.52, 1994.
2. C.R. Stillwell, Recent Advances in Porometry and Porosimetry: Introducing the Microflow Porometer and the Aquapore Porosimeter, Proceedings of the 7^{th}. World Filtration Congress, Budapest. Hungary, 1996.
3. Vibhor Gupta and A.K. Jena, Substitution of Alcohol in Porometers for Bubble Point Determination, Advances in Filtration and Separation Technology, Volume 13b, pp.833-44, American Filtration and Separation Society, 1999.
4. K. Denbigh, The Principles of Chemical Equilibrium, Cambridge University Press, London, 1968.
5. Akshaya Jena and Krishna Gupta, In-plane Compression Porometry of Battery Separators, Power Source 17, Ed. A. Attewell, Elsevier, PP.46, 1999.
6. A.W. Adamson, Physical Chemistry of Surfaces, Inter Science, New York, 1967.
7. A. E. Scheidegger, The Physics of Flow through Porous Media, Macmillan, New York, 1957.

CHARACTERIZATION OF PORE STRUCTURE OF ELECTRODES OF SOLID OXIDE FUEL CELLS

Akshaya Jena and Krishna Gupta
Porous Materials, Inc.
20 Dutch Mill Road
Ithaca, NY 14850

ABSTRACT

In this paper, the pore structure characteristics of two considerably different ceramic electrode materials were successfully investigated using flow porometry. Through pore throat diameters, distribution of flow rate over pore diameters and gas permeability were measured. Pore volumes measured with mercury intrusion porosimetry showed that the through pores and the blind pores were associated with considerable volume of wide parts. The results were consistent with scanning electron micrographs.

INTRODUCTION

Electrodes tend to be porous in order to permit flow of reactants, facilitate electrode reactions and permit flow of products. The important pore structure characteristics of electrodes include through pore diameters, through pore size distribution, through pore surface area, and gas permeability. Control of such pore structure characteristics is possible through process control parameters such as characteristics of starting material, forming methods, sintering temperature and sintering time. Therefore, it is important to be able to accurately measure the pore structure characteristics of electrodes of solid oxide fuel cells.

CHARACTERIZATION TECHNIQUE

Flow Porometry

For capillary flow porometry, pores of the sample are spontaneously filled with a wetting liquid and pressure of a non-reacting gas is increased on the sample to empty the pores and permit gas flow. Differential gas pressure needed for displacement of the wetting liquid in a pore is related to pore size[1].

$$p = 4 \gamma \cos \theta / D \qquad (1)$$

where p is the differential gas pressure across the pore, γ is the surface tension of the wetting liquid, θ is the contact angle of the wetting liquid, and D is the pore diameter. For pores of irregular cross-section, pore diameter, D, is defined by Equation 2.

$$[(\text{Perimeter}) / (\text{Area})]_{\text{pore}} = [(\text{Perimeter}) / (\text{Area})]_{\text{circular opening of diameter, D}} = 4 / D \qquad (2)$$

Differential gas pressure and flow rates through a dry sample and the same sample with its pores filled with a wetting liquid are measured. Various pore structure characteristics

including largest through pore throat diameter, mean through pore throat diameter, pore distribution, and gas permeability are computed from measured values.

The instrument used in this investigation is shown in Figure 1. The instrument was fully automated in order to obtain accurate data. Test execution, data acquisition, data storage and data reduction were conveniently carried out using Windows based soft ware. The instrument accurately measured flow rates and pore sizes over a wide range. The special design of the instrument permitted measurement of very small flow rates through some of the dense electrodes. It was possible to test samples having a variety of shapes and sizes.

Figure 1. The Microflow Porometer used in this investigation

Mercury Intrusion Porosimetry

A nonwetting liquid like mercury cannot enter pores spontaneously. Increase of pressure on mercury forces mercury into pores. The pressure is related to pore diameter[2].

$$D = - 4 \gamma \cos \theta / p \qquad (3)$$

where D is pore the diameter defined by Equation 2, γ is the surface tension of the nonwetting liquid mercury, θ is the contact angle of mercury, and p is the intrusion pressure. Intrusion volume and intrusion pressure are measured. Intrusion pressure gives diameter and intrusion volume gives pore volume of through and blind pores.

The mercury intrusion porosimeter used in this investigation is shown in Figure 2. The special design of the instrument prevented exposure to mercury. The test execution, data acquisition and data reduction were fully automated for accurate data.

Materials

Samples of materials for several components of SOFC were investigated. One was NiO-YSZ. The other was a two-phase composite of two oxides. The composites I and II contained different percentages of nickel oxide.

RESULTS AND DISCUSSIONS

Through Pore Throat Diameters

Capillary Flow Porometry detects the presence of a pore when the wetting liquid is completely removed from the pore and gas starts flowing through the pore. The differential

pressure at which a pore becomes completely empty is the pressure required to displace the wetting liquid from the pore throat because this is the maximum pressure needed to remove liquid from the pore (Equation 1). Therefore, the pore diameter computed from the differential pressure at which gas flow starts through a pore is the pore throat diameter (Figure 3).

Figure 2. The Mercury Intrusion Porosimeter used in this investigation

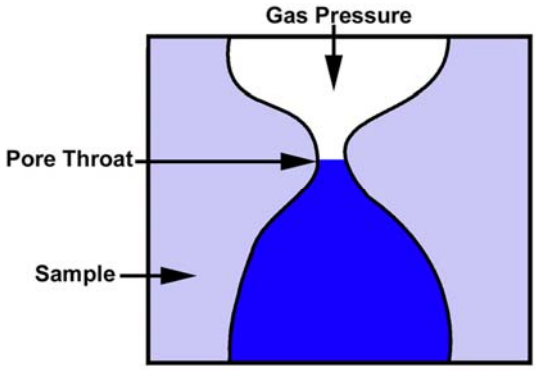

Figure 3. Pore diameters measured by flow porometry

In order to measure the through pore throat diameters, the ceramic components were tested by flow porometry. Such components are likely to contain blind pores. Therefore, the samples were evacuated, completely wetted with the wetting liquid galwick having a surface tension of 16 dynes/cm and tested in microflow porometer capable of measuring very low flow rates. The flow rates through wet and dry samples as functions of differential pressure are shown in Figure 4.

The pore throat diameters are computed from the measured differential pressure. The largest through pore throat diameter is computed from pressure to initiate flow through wet sample. The mean flow through pore throat diameter is obtained from the mean flow pressure. The mean flow pressure is the pressure at which the flow through the wet sample becomes equal to the half-dry flow (Figure 4). The half-dry flow is half of the flow through the dry sample at any pressure. The range of measured through pore throat diameters of two materials designed for SOFC are listed in Table I.

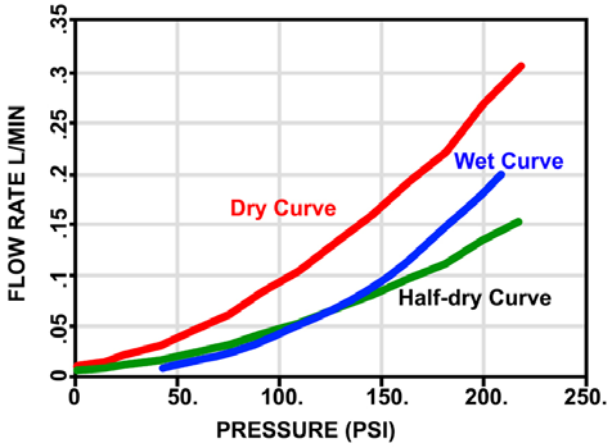

Figure 4. Variation of air flow rate with the differential pressure through YSZ (PSI =6.895 kPa)

Table I. Throat diameters of through pores

	The largest pore, μm	The mean flow pore, μm
YSZ	0.151	0.053
Composite I	487	237

Flow Distribution Over Through Pore Throat Diameters

Flow distribution over through pore throat diameters is determined by the number of different diameter pores. Flow distribution is given by distribution function**,** f:

$$f = - d[(F_w/ F_d)\times 100] / dD \qquad (4)$$

where F_w and F_d are flow through wet and dry samples respectively. The flow distribution in the composite II is shown in Figure 5. The distribution function in this figure is normalized taking the maximum value of the function to be 100. The area under the function in any pore diameter range is proportional to the percentage of flow in that diameter range. Pores with appreciable contribution to flow are listed in Table II. The distribution function can also yield the fractional pore number distribution.

Table II. Pores with appreciable contributions to flow

Material	Distribution	Diameter range, μm
YSZ	Narrow, Bimodal	0.04 – 0.08
Composite I	Broad, Unimodal	50 – 250

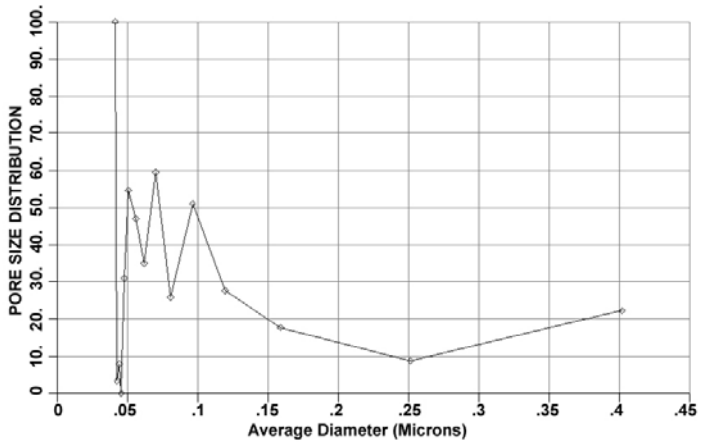

Figure 5. Flow distribution over through pore throat diameters in composite II

The pore structures of the ceramic electrode materials may be noted from their Scanning Electron Micrographs (Figure 6). The measured pore diameters are consistent with the micrographs. Pores in YSZ are much smaller than those in the composite.

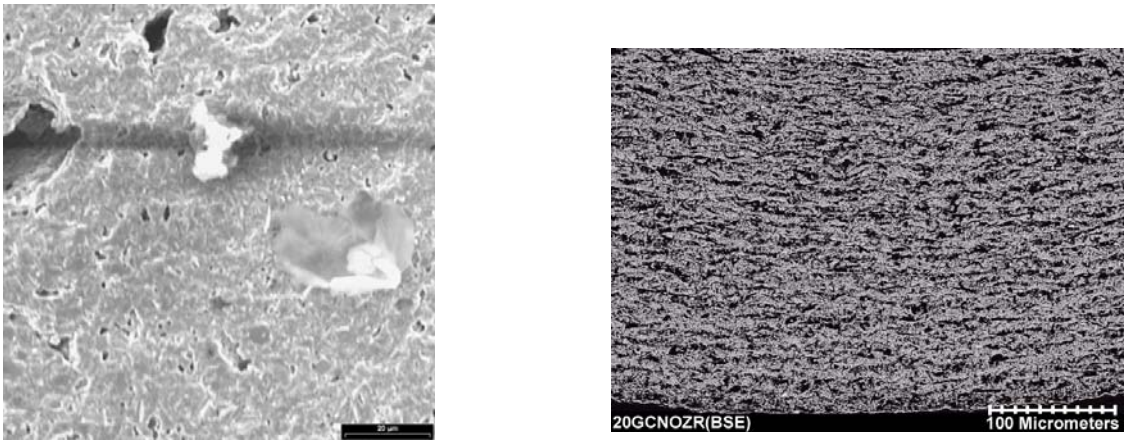

(a) (b)

Figure 6. SEM micrographs of ceramic electrode materials, (a) YSZ and (b) Composite

All Diameters of Through and Blind Pores

Each pore normally has many pore diameters. All diameters of through and blind pores are measured by intrusion porosimetry (Figure 7). The measured pore diameters are shown in Figure 8.

Volume of Through and Blind Pores

As illustrated in Figure 7 volumes of through and blind pores are measurable by mercury intrusion porosimetry. The results of YSZ are illustrated in Figure 8.

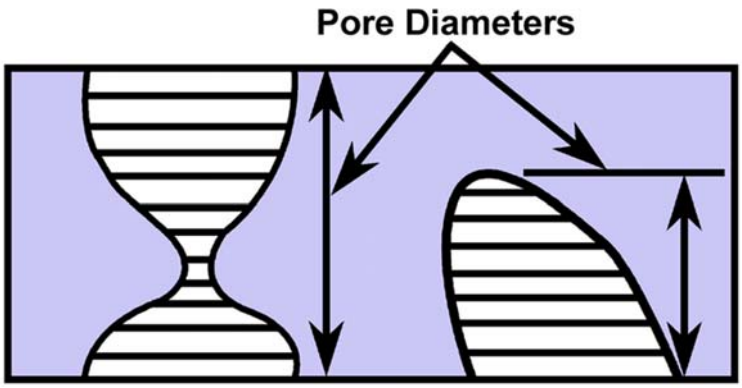

Figure 7. Diameters and volumes of through and blind pores measured by intrusion porosimetry

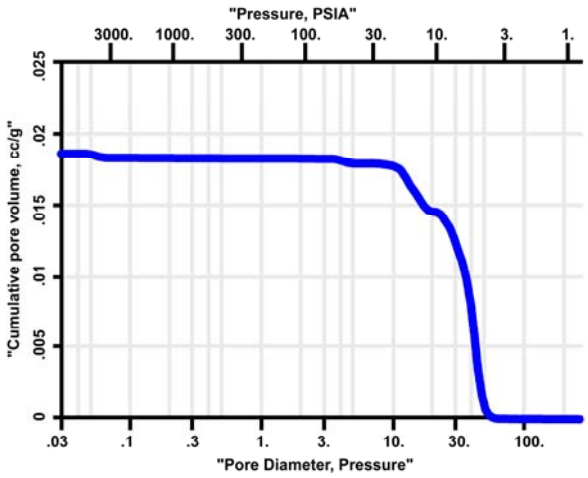

Figure 8. All diameters of pores and volumes of through and blind pores in YSZ

Distribution of Pore Volume Over Through and Blind Pore Diameter

Volume distribution over pore diameters is given in terms of the distribution function, fv;

$$fv = - (dV/d \log D) \quad (5)$$

where V is the pore volume. Distribution of through and blind pore volume over their diameters in YSZ is shown in Figure 9. The area under the function in any pore size range gives volume of pore in that range. Several pore peaks can be seen in the distribution curve.

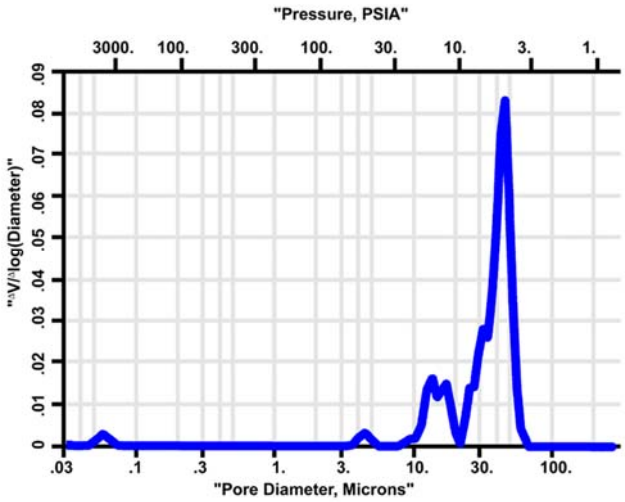

Figure 9. Distribution of volume of through and blind pores over their diameters in YSZ

Shape of Through Pores

Contributions to pore volumes by pores of different sizes obtained from the pore peaks of YSZ are listed in Table III. The through pores in YSZ have throat diameters close to 0.05 μm and have very small pore volumes associated with pore throats. This result is consistent with the small gas flow rates (0.05 l/min) through YSZ (Figure 4). The measured large pore diameters and large volumes must be associated with the wide mouths of through pores and blind pores. The presence of such pores in YSZ is seen in the SEM in Figure 6.

Table III. Contributions to pore volumes by pores of different sizes

Pore diameter	Pore volume
~ 40 μm	79 % Pore Volume
~ 15 μm	17 % Pore Volume
~ 4.5 μm	2.5 % Pore Volume
~ 0.06 μm	1.5 % Pore Volume

Permeability

Gas permeability was calculated from gas flow rate through dry sample using Darcy's law.

$$\underline{F} = - [k A / \mu] (dp /dx) \qquad (6)$$

where k is permeability, $\underline{F}$ is flow rate in volume at average pressure and test temperature, A is area of the sample, μ is viscosity of fluid, and (dp/dx) is pressure gradient across the sample. Flow rates are measured in terms of flow, F, at standard temperature and pressure. Expressing $\underline{F}$ in terms of F and integrating over the thickness of the sample;

$$F = k [(A T_{s)} / (2 \mu l p_s T)] [pi^2 - p_0^2] \qquad (7)$$

where T_s is standard temperature, l is thickness of sample, p_s is standard pressure, T is experimental temperature, p_i is inlet pressure, and p_0 is outlet pressure. Gas flow rates measured through the composite II as functions of differential is shown in Figure 10. The calculated air permeability of the composite is 9.96×10^{-3} Darcies. Permeability could also be expressed in any other unit including Frazier, Gurley and Rayle.

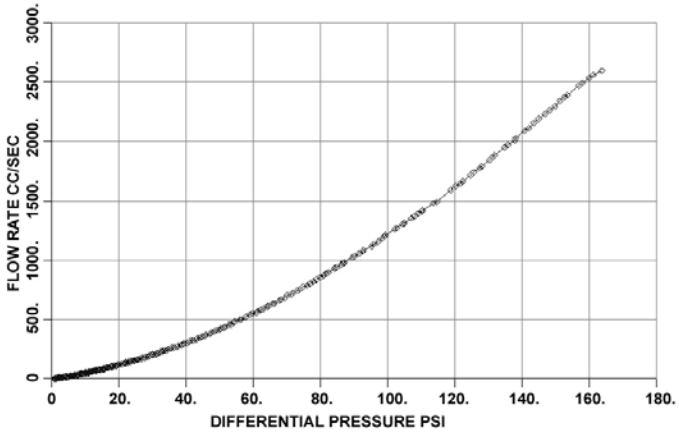

Figure 10. Variation of airflow rate through the composite II as a function of pressure

SUMMARY AND CONCLUSION

The pore structure characteristics of two materials developed for SOFC, were investigated by capillary flow porometry. The pore structure characteristics, through pore throat diameters, the largest through pore throat diameter, mean flow through pore throat diameter, flow distribution over pore diameter, pores exhibiting appreciable flow, and gas permeability were successfully measured.

YSZ exhibited very low flow, a bimodal distribution, the largest through pore throat diameter of 0.151 μm, mean flow through pore throat diameter of 0.053 μm, and pore diameters of 0.04–0.08 μm exhibiting appreciable flow. Composite I exhibited a broad unimodal distribution, the largest through pore throat diameter of 487 μm, mean flow through pore throat diameter of 237 μm, and pore diameters of 50-250 μm exhibiting appreciable flow. In composite II, the distribution peak was observed at 0.05-0.12 μm and the permeability was 9.96×10^{-3} Darcies.

REFERENCES

[1]Akshaya Jena and Krishna Gupta, "Liquid Extrusion Techniques for Pore Structure Evaluation of Nonwovens," *International Nonwovens Journal*, Fall, 45-53 (2003).

[2]Akshaya Jena and Krishna Gupta, "Characterization of Pore Structure of Filtration Media," *Fluid particle Separation Journal*, **14**, 227-241 (2002).

Second International Conference on
Fuel Cell Science, Engineering and Technology

FuelCell 2004 –xxxx

CHARACTERIZATION OF WATER VAPOR TRANSMISSION RATE THROUGH FUEL CELL COMPONENTS

Akshaya Jena, Krishna Gupta, and Matthew Connolly

Porous materials, Inc., 20 Dutch Mill Road, Ithaca, NY 14850, USA, E-mail: info@pmiapp.com

ABSTRACT

An instrument capable of measuring vapor transmission rates under any desired gradient of concentration and pressure is described. The test temperature, pressure, humidity and flow rates are precisely controlled and accurately measured. The instrument is completely automated to obtain objective and accurate results and minimal involvement of the operator. Using this instrument a variety of materials, including a fuel cell component, have been successfully investigated.

INTRODUCTION

The rate of water vapor transmission through fuel cell components is a critical parameter that determines the performance of the fuel cell. Water vapor transmission can be a very complex process (Jena and Gupta, 2002). The component might react with the water vapor, swell and cause many physical property changes. The vapor might migrate through small pores in the component or diffuse through the material. One of the examples is water vapor transmission through nafion membrane under a pressure gradient (Jena and Gupta, 2002). Presence of concentration gradient, presence of pressure gradient, presence of temperature gradient or simultaneous presence of some of the gradients could drive the vapor transmission process. A technique has been developed, and an instrument has been fabricated, to measure vapor transmission rates under controlled conditions in which all the variables can be independently controlled. Water vapor transmission rates through a variety of materials have been investigated. A fuel cell component has been investigated, and water vapor transmission rate through the component has been successfully determined as a function of average humidity at a constant humidity gradient.

TECHNIQUE

Basic Principle

When a gas containing water vapor flows below as well as above a sample, vapor transport through the sample can occur due to an imposed concentration or pressure gradient. Consider mass balance in the chamber in to which vapor is transported through the sample. The rates of addition of water vapor by the incoming gas and by the transport through the sample must be equal to the rate of removal of water vapor by the outgoing gas under steady state conditions (Figure 1).

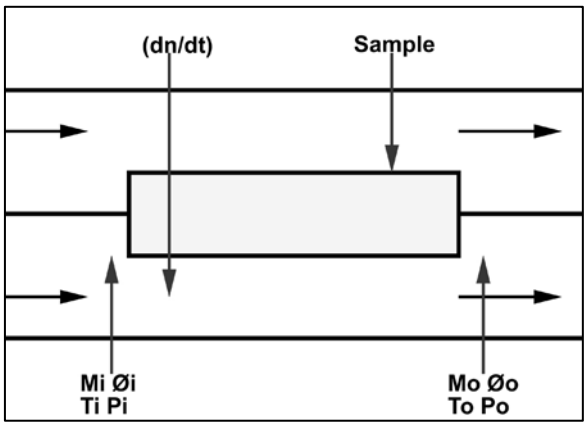

Fig. 1 Basic principle of the technique

$$(dn/dt) + [(p_{e,i}\phi_i / P_i)\, M_i] = [(p_{e,o}\phi_o / P_o)\, M_o] \qquad (1)$$

Where
dn/dt = Rate of vapor transport in moles

p_e = equilibrium vapor pressure at temperature, T and total pressure, P.
ϕ = humidity = (p_v/p_e)
p_v = partial pressure of vapor in unsaturated gas
M = Rate of gas flow in moles
$_i$= incoming flow
$_o$= outgoing flow
Vapor transport rate is computed from known T, P, ϕ and M.

Technology

The outline of the instrument designed for this study is shown in Figure 2. The sample is contained in a holder. Two gas streams are allowed to flow independently on both sides of the sample. A part of the gas flowing through each stream is allowed to go through bubblers while the other part bypasses the bubblers and mixes with the gas passing through the bubblers. The flow rate of each part of the gas is controlled and measured by flow controllers. The humidity and temperatures of gas streams are measured. The differential pressure between both sides of the sample is measured. Two valves are provided at the outlet ends of the gas streams. The sample holder and all the attachments are maintained at a constant temperature.

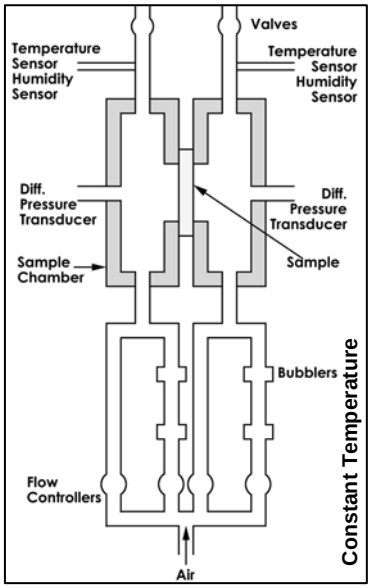

Fig. 2 Outline of the setup

The apparatus is enclosed in a constant temperature chamber whose temperature is monitored. The temperatures of the gas streams on the two sides of the sample are also constantly monitored to see if there is appreciable temperature fluctuation because of reaction of the vapor with the sample.

The humidity of the gas entering any one side of the sample is controlled by mixing the gas bypassing the bubblers with the gas going through the bubblers. Gas going through the bubblers is saturated with water vapor. Saturation vapor pressure is a function of temperature and total pressure. Assuming water vapor at the constant temperature to behave like an ideal gas:

$$p_{e(P)} = p_{e(P=1)} \exp [(V_L(P-1) /RT] \quad (2)$$

where V_L is molar volume of liquid, P is pressure in atmospheres, T is absolute temperature and R is the gas constant. This equation suggests that the error in p_e is about 0.075 % at two atmosphere pressure. At high pressures, water vapor does not behave like an ideal gas. The errors in p_e due to non-ideal behavior is about 0.7 % at two atmosphere pressure (Hayland, 1975). Therefore, to minimize errors, the total pressure is measured and kept close to one atmosphere. p_e is either measured or taken from literature.

Desired humidity in the incoming gas is obtained by automatically manipulating the flow through flow controllers. Under the test condition of constant temperature and close to one atmospheric pressure, water vapor is expected to show ideal behavior. Consequently, the humidity, ϕ in the incoming gas is given by:

$$\phi = (p_v / p_e) = 1 / \{1+[n_2/n_1][1-(p_e /P)]\} \quad (3)$$

Where n_1 and n_2 are molar flow rates of gas through bubblers and bypassing the bubblers respectively. Thus, the desired value of ϕ is maintained by maintaining a constant ratio (n_2/n_1) for known values of p_e and P. It was possible to maintain as high as 95 % humidity.

Vapor from gas on one side of the sample diffuses through the sample and is transported to the gas on the other side. Therefore, humidity of the outgoing gas on one side of the sample will be reduced while that on the other side will increase. The humidity of the outgoing gas on both sides of the sample is directly measured.

The average humidity in the incoming and outgoing gases on one side of the sample yields the average humidity on that side. The difference between the average humidity is the driving force for vapor transport.

The pressure is controlled by the valve at the end of each gas flow line. A differential pressure transducer continuously records the pressure difference across the sample. The valves are automatically controlled to maintain either zero differential pressure or a definite pressure difference.

Flow rates of outgoing gas on both sides of sample are directly measured. Consideration of mass balance suggests that,

$$M_o = M_i + (dn/dt) \quad (4)$$

Water vapor transmission rate through the sample is obtained from Eqs. (1) and (4). During the test, T is a constant. p_e, $p_{e,o}$ and $p_{e,i}$ are equal and are in atmospheres. P, P_o and P_i are one atmosphere each. Hence,

$$(dn/dt) = [p_e\phi_o - p_e\phi_i] M_o / [1 - p_e\phi_i] \quad (5)$$

All the parameters required for computing vapor transmission rate using Eq. (5) are measured.

RESULTS AND DISCUSSION

Plastic sheet

In order to test the equipment a plastic sheet with very low porosity was used as the sample. Water vapor transmission rates were measured as functions of applied humidity. The water vapor transmission rate at a humidity difference of 0.5 across the sample was measured as a function of average humidity. The data are listed in Table 1. Although the variation of transmission rate with humidity is very small, it is detectable as shown in Figure 3. The very small vapor transmission rate is in excellent agreement with the very low porosity of the plastic sheet.

Table 1. Water vapor transmission rate through a plastic sheet of very low porosity

Relative humidity, %			Flux of water vapor, kg/m^{2}s
Top	Bottom	Average	
55	5	30	2.81 E-07
65	15	40	5.99 E-07
75	25	50	4.87 E-07
85	35	60	7.60 E-07
95	45	70	1.27 E-06

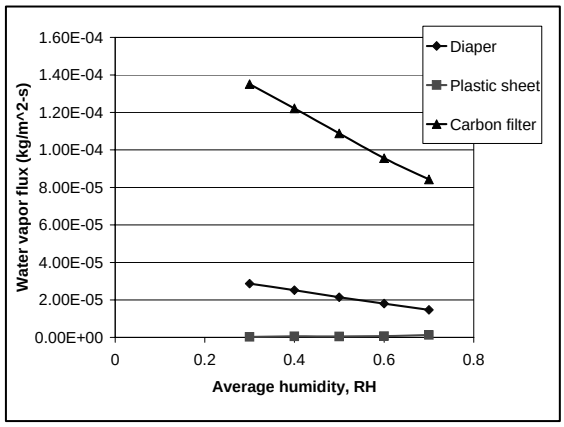

Fig. 3 Variation of water vapor transmission rate through a number of materials as a function of average humidity

Diaper and carbon filter

Two other materials were tested in order to further examine the capability of the equipment. A diaper having higher permeability than the plastic sheet was examined. The results are shown in Figure 3. The transmission rate of about 2×10^{-5} kg/m^{2}s is reasonable for the diaper. A carbon filter with an order of magnitude higher transmission rate was also examined. The vapor transmission rate through the carbon filter is shown in Figure 3 as a function of average humidity at a constant humidity difference of 0.5. The result is in the expected range.

Fuel cell component

The cathode component of a leading fuel cell developer was tested in the equipment for water vapor transmission rate. The temperature was kept constant at 25°C. The pressure gradient was kept at zero. Humidity was varied between 0.95 and 0.55 in the top chamber and between 0.45 and 0.05 in the bottom chamber. The water vapor transmission rate was computed in kg/m^{2}s. The results are listed in Table 2.

Table 2. Water vapor transmission rate through the cathode component of a fuel cell

Relative humidity, %			Flux of water vapor, kg/m^{2}s
Top	Bottom	Average	
55	5	30	1.41E-04
65	15	40	1.13E-04
75	25	50	1.02E-04
85	35	60	9.11E-05
95	45	70	7.77E-05

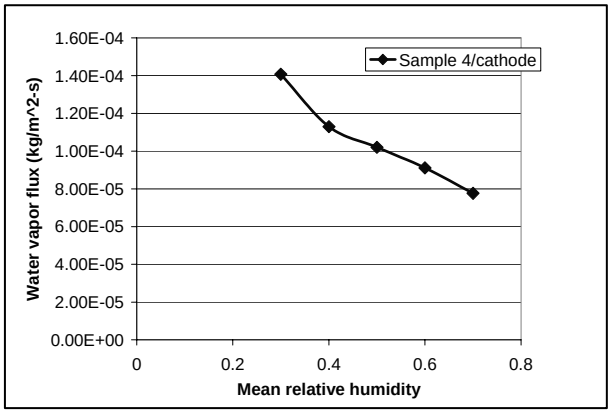

Fig. 4 Water vapor transmission rate through the cathode component of a fuel cell

The variation of water vapor transmission rate through the cathode component is shown in Figure 4. The variation

is nonlinear. This is unlike the behavior of other materials (Figure 3). The water vapor transmission rate through the cathode material increases with increasing rate with decrease in average humidity. The interaction of the cathode material tends to change with changing humidity. The material could physically interact with water vapor in many possible ways. The vapor may be absorbed, the material may swell, pore shape and size may change and vapor may condense in some of the pores.

SUMMARY AND CONCLUSION

1. An instrument has been designed with potential to determine water vapor transmission rates through fuel cell components at the desired temperature under a range of humidity gradients at any desired average humidity, and a range of pressure gradients. The instrument is fully automated.
2. A plastic sheet with very low permeability was examined to test the system. As expected the instrument gave very low vapor permeability.
3. A diaper and a carbon filter were also investigated in order to test the capability of the instrument. The results were satisfactory.
4. A fuel cell cathode component was tested at 25° C keeping the pressure gradient zero and varying the average humidity over a wide range at a constant humidity gradient. The instrument yielded satisfactory results over the wide range of humidity.
5. It is proposed to continue testing a variety of fuel cell components under humidity as well as pressure gradients in order to further evaluate the instrument.

ACKNOWLEDGEMENTS

The instrument described in this paper was developed on the basis of the methodology demonstrated by Phillip Gibson of U.S. Army Soldier Systems Center, Natick, Massachusetts. Some of the data presented here were obtained using the prototype DMPC developed by the Army. We are grateful to him for his advice and help.

REFERENCES

Hayland, R. W., 1975, A Correlation for the Second Interaction Varial Coefficient and Enhancement Factor for Moist Air, *J Research NBS, A. Physics and Chemistry*, Vol. 79A, pp. 551-560.

Jena, Akshaya, and Gupta, Krishna, 2002**,** A Novel Technique for Determination of Vapor Transmission Rate through Textiles', *Journal of Industrial Textiles,* Vol. 31, Number 4, pp. 273-281.

Jena, Akshaya, and Gupta, Krishna, 2002, Characterization of Water Vapor Permeable Membranes, *Desalination*, Vol. 149, pp. 471- 476.